KAERI/TR-1580/2000

기술보고서

소듐 이상유동 모델 'SOBOIL' 개발

Development of Two-phase Flow Model, 'SOBOIL', for Sodium

2000. 6.

한 국 원 자 력 연 구 소

KOREA ATOMIC ENERGY RESEARCH INSTITUTE

Please be aware that all of the Missing Pages in this document were originally blank pages

제 출 문

한국원자력연구소장 귀하

이 보고서를 2000 년도 "액체금속로 안전해석 기술개발" 과제의 기술보고서로 제출합니다.

2000년 6 월 9 일

과제명 : 액체금속로 안전해석
기술개발

주저자 : 장 원 표

공저자 : 김 인 철

권 영 민

이 용 범

한 도 희

요 약 문

I. 제목

소듐 이상유동 모델 SOBOIL 개발

II. 연구목적 및 중요성

본 연구는 KALIMER HCDA(Hypothetical Core Disruptive Accident) 초기 단계를 평가에 필요한 소듐 이상유동 해석모델 개발을 목적으로 한다. 사고 초기의 노심용융 및 사고전개는 주로 노심 반응도에 의해 결정되며, 노심 반응도 효과는 기포분포에 의해 결정적 영향을 받는다. 이 때문에 노심내 기포 분포에 대한 정확한 예측은 사고전개 예측의 불확실성을 감소시켜 궁극적으로는 안전여유도 및 해석의 신뢰도 증대효과를 가져올 수 있다.

따라서 소듐 이상유동 모델 개발과 이에 대한 해석체계 확보는, 현재까지 국내에서 관련 모델이나 해석체계가 확보되지 못한 상태이므로, 최종 KALIMER 설계의 안전성 입증에 필수적이라 할 수 있다.

III. 연구내용 및 범위

본 연구에서 개발되는 소듐 이상유동 모델, 'SOBOIL'은 기본적으로 SAS2A[1]에 사용된 Multi-bubble Slug Ejection 모델과 유사하다. 이 모델에서는 기포가 발생하면 기포는 피복재 혹은 구조물의 얇은 액체막을 제외한 전체 유로 단면적을 채우며, 액체 Slug에 의해 분리되는 것으로 가정한다. 한 유로 내에서는 최대 9개까지의 기포가 동시에 존재하는 것을 허용한다.

이 모델에서 각 액체 Slug 유동량 계산은 2단계로 수행되는 데, 첫 단계로 기포의 압력이 변하지 않는 것으로 가정하고 초기 유동량을 먼저 계산한다. 이 과정에서 액체 Slug의 온도 및 압력 분포, 그리고 액체와 기포사이의 경계면 속도도 함께 계산된다. 다음으로 기포로 전달되는 순 에너지와 기포의 내부 에너지 변화의 균형으로부터 새로운 기포의 온도 및 압력이 계산된다. 기포내로의 순에너지 전달은 액체/기포 경계면에서의 계면 열전달과 벽면 열전달로 구성되어 있으며, 기포 에너지 변화는 기포 응축, 기포 온도변화, 그리고 액체막의 기화에 의해 결정된다.

새로운 기포압력이 결정되면 압력변화를 고려하여 최종 액체 Slug의 유동량이 계산되며 이 방법으로 계산을 반복한다.

IV. 연구결과 및 활용에 대한 건의

현재 SOBOIL은 구성 세부모델들간 상호 연계가 확인되었고, 현상 예측을 위한 개략적인 논리는 완성되었다. 이에 따라 전형적인 이상유동 현상의 예측은 가능해졌지만, 모델의 일반적인 타당성과 가정의 정당성 등에 대해서는 충분히 확인되지 못했다. 이런 이유로 경우에 따라 세부적 모델에 고려되지 못했던 현상 혹은 논리의 취약점에 기인해서 해의 불안정성이 발생할 가능성을 배제할 수 없다.

따라서 개발된 모델이 신뢰할 수 있는 예측모델로 발전하기 위해서는 상당 기간의 시험과 개선을 통한 검증이 필요하다. 이를 위해 국내에서 부재한 검증 참조 모델 혹은 실험자료를 확보하기 위해 관련 국제협력에 더욱 관심을 기울여야 할 것으로 사료된다.

S U M M A R Y

I. Project Title

Development of Two-phase Flow Model, 'SOBOIL', for Sodium

II. Objective and Importance of the Project

The objective of this research is to develop a sodium two-phase flow analysis model for the assessment of the initial stage of the KALIMER HCDA (Hypothetical Core Disruptive Accident). The early core melting and the accident development largely depend on the reactivity, and the reactivity effect is affected by the void distribution in the core. The accurate prediction of the sodium void distribution in the core may reduce the uncertainties involved in the accident evolution, and, thus, it eventually brings the enhancement of both safety margin and analysis reliability.

Therefore, it is considered that development of a sodium two-phase model as well as establishment of the related analysis system, must be very important for demonstration of the ultimate KALIMER design safety, because they are still unavailable in Korea.

III. Scope and Contents of Project

The present developing model, 'SOBOIL', is basically similar to the multi-bubble Slug Ejection model used in SAS2A[1]. When a bubble is formed within the liquid slug, the bubble fills the whole cross section of the coolant channel except for a film left on the cladding or on the structure. Up to nine bubbles, separated by the liquid slugs. are allowed in the channel at any time.

Each liquid slug flow rate in the model is performed in 2 steps. In the first step, the preliminary flow rate in the liquid slug is calculated neglecting the effect of changes in the vapor bubble pressures over the time step. The temperature and pressure distributions, and interface velocity at the interface between the liquid slug and vapor bubble are also calculated during this process. The new vapor temperature and pressure are then determined from

the balance between the net energy transferred into the vapor and the change of the vapor energy. The net energy transfer into the vapor consists of the interfacial heat transfer and wall heat transfer. Meanwhile, the vapor condensation, temperature change, and vaporization from the liquid film contribute to the vapor energy change.

The liquid flow is finally calculated considering the change of the vapor pressure over a time step and the calculation is repeated until specified elapsed time is met.

IV. Results and Proposal for Application

As results of the present study, coupling between the sub-models in 'SOBOIL' has been confirmed and overall calculation logic for representing the physical phenomena has been accomplished as well. The prediction of the typical phenomena is now possible, but sufficient validation on the calculational algorithm as well as the validity of the assumptions used in the model has not been made yet. For this reason, unexpected unstable solutions may be obtained, due to a model or logic defect not considered in the present model.

Continuous effort, therefore, must be made on the examination and improvement for the model to become reliable. To this end, much interest must be concentrated in the relevant international collaborations for access to a reference model or test data for the verification.

Table of Contents

Chapter 1 Theory for Sodium Boiling Model (SOBOIL)

Chapter 2 SOBOIL Structure

Chapter 1 Theory for Sodium Boiling Model (SOBOIL)

1. Introduction

Sodium boiling model in the SOBOIL is basically Multi-bubble Slug Ejection model similar to that used in SAS2A.[1] Changes have been made in the finite differencing to handle the area change and non-uniform axial node more consistently. In addition, it has been modeled with a more general approach in calculation of the conduction heat transfer for the fuel rod and the structure. Figure 1 represents the nodalization for numerical method used in SOBOIL. Voiding is assumed to result in formation of bubbles that fill the whole cross section of the coolant channel except for a film left on the cladding or on the structure. Up to nine bubbles, separated by liquid slugs, are allowed in the channel at any time. The liquid film around the vapor is assumed to be static currently, its motion, however, will be improved later.

The present model is summerized as the following 3 steps in the calculation:

(1) Extrapolation for calculations of the temperature distributions and flow rates in the liquid slugs
- Calculations of the temperature distribution and flow rate in each liquid slug separated by bubbles with neglecting the effect of changes in the vapor bubble pressures over the time step

(2) Calculations of the advanced time pressures and mass flow rates using extrapolated physical properties as well as the pre-estimated flow rates

(3) Calculation of the advanced vapor temperatures

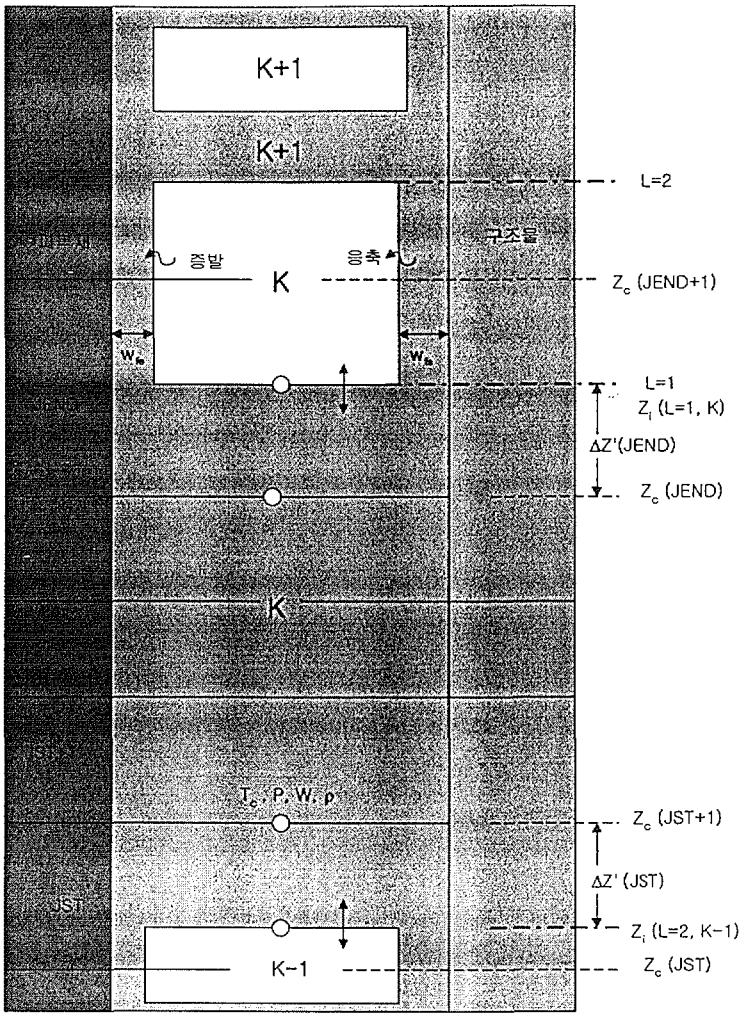

Fig. 1 Channel Nodalizations for 'SOBOIL' Model

2. Liquid Slug Flow Rates

The description of the momentum conservation equation for the liquid flow is similar to that used in SAS2A, except expressing it with the flow rate instead of mass flux in order to take account of the flow area variation for a node in the numerical computation. The liquid momentum equation is given by

$$\frac{1}{A_c}\frac{\partial W}{\partial t} + \frac{\partial P}{\partial z} + \frac{1}{A_c}\frac{\partial (Wv)}{\partial z} = -\left(\frac{\partial P}{\partial z}\right)_{fr} - \left(\frac{\partial P}{\partial z}\right)_{K} - \rho_c g \tag{1}$$

The momentum equation is applied to each slug which is represented in the figure 1, individually, and is integrated over the length of each slug rather than over the length of the channel, then one can obtain

$$I_1 \frac{\partial W}{\partial t} + P_t - P_b + W^2 I_2 + A_{fr} W|W|^{1+b_{fr}} I_3 + W|W| I_4 + g I_5 = 0 \tag{2}$$

where

$$I_1 = \int \frac{dz}{A_C} = \sum_{JC=JST}^{JEND} X_{I1}(JC) \tag{3}$$

$$X_{I1}(JC) = \frac{\Delta z(JC)}{A_C(JC)} \tag{4}$$

$$I_2 = \sum_{JC=JST}^{JEND} X_{I2}(JC) \tag{5}$$

$$X_{I2}(JC) = \frac{1}{A_C(JC)^2}\left[\frac{1}{\rho_C(JC+1)} - \frac{1}{\rho_C(JC)}\right] \tag{6}$$

$$I_3 = \int \frac{1}{2\rho_C A_C^2 D_h}\left[\frac{D_h}{\mu A_C}\right] b_{fr}\, dz = \sum_{JC=JST}^{JEND} X_{I3}(JC) \tag{7}$$

$$X_{I3}(JC) = \frac{\Delta z(JC)}{\left[\rho_C(JC) + \rho_C(JC+1)\right] A_C(JC)^2 D_h(JC)} \left[\frac{D_h(JC)}{\overline{\mu}(JC) A_C(JC)}\right]^{b_{fr}} \tag{8}$$

$$I_4 = \sum_{JC=JST}^{JEND} K_{OR}(JC) \tag{9}$$

$$I_5 = \int \rho_C \, dz = \sum_{JC=JST}^{JEND} X_{I5}(JC) \tag{10}$$

$$X_{I5}(JC) = 0.5 \left[\rho_C(JC) + \rho_C(JC+1)\right] \Delta z(JC) \tag{11}$$

P_b = the pressure at the bottom of the Slug, and

P_t = the pressure at the top of the slug

The integer variable JST is the number of the mesh segment in which the bottom of the liquid slug is located, while JEND is the number of the segment in which the top is contained. Since the integration is over only the liquid portions of these segments, the axial length terms Δz (JC) in the expressions for X_{I1}, X_{I3}, and X_{I5} must be altered as follows :

$$If \quad K > 1 \quad \Delta_z'(JST) = z_C(JST+1) - z_i(L=2,\ t,\ K-1)$$

$$If \quad K = 1, \quad \Delta z'(JST) = \Delta z(JST)$$

$$If \quad K < K_{vn}, \quad \Delta z'(JEND) = z_i(L=1,\ t,\ K) - z_c(JEND)$$

$$If \quad K > K_{vn}, \quad \Delta z'(JEND) = \Delta z(JEND)$$

where Z_i (L, t, K) denotes the location of the interface between the liquid and the vapor, 1 for the lowest bubble in the channel, and K_{vn} for the highest bubble.

Two other nodes must be modified to describe the partial segments at the ends of the slug. If JST = 1, the effective inertia term $\left(\frac{\Delta Z_i}{A}\right)_b$ must be added to I_1, and if JEND = MZD (the last node), $\left(\frac{\Delta Z_i}{A}\right)_t$ must be included in the calculation of I_1.

In the special case of a small liquid slug entirely contained within one mesh segment, JST = JEND. Then,

$$\Delta z'(JST) = z_i\,(L=1,\ t,\ \mathrm{K}) - z_i\,(L=2,\ t,\ \mathrm{K}-1)$$

and there is only one term in each of the summations for I_1 through I_5 . To allow flexibility in the level of implicitness of the calculation, the variable Explicit/Implicit Scheme is applied to the coefficients in Eq. (2) as the similar manner as used in SAS2A. The final differenced equation is then,

$$\begin{aligned}
&\left(\theta_1 \mathrm{I}_1\,|_t + \theta_2 \mathrm{I}_1\,|_{t+\Delta t}\right)\frac{\Delta W}{\Delta t} + \theta_1\,(Pt_1 - Pb_1) + \theta_2\,(Pt_2 - Pb_2) \\
&+ \left(\theta_1 \mathrm{I}_2\,|_t + {}_2\mathrm{I}_2\,|_{t+\Delta t}\right)\left(W_1^2 + 2\theta_2 W_1 \Delta W\right) + \mathrm{A}_{fr}\left(\theta_1 \mathrm{I}_3\,|_t + \theta_2 \mathrm{I}_3\,|_{t+\Delta t}\right) \\
&\left[W_1\,|W_1|1+b_{fr} + {}_2\left(2+b_{fr}\right)|W_1|1+b_{fr}\ \Delta W\right] + \left(\theta_1 \mathrm{I}_4\,| + \theta_2 \mathrm{I}_4\,|_{t+\Delta t}\right) \\
&\left(W_1\,|W_1| + 2\theta_2 |W_1|\Delta W\right) + \left(\theta_1 \mathrm{I}_5\,|_t + \theta_2 \mathrm{I}_5\,|_{t+\Delta t}\right) g = 0
\end{aligned} \tag{12}$$

All I's in Eq. (12) except I_5 are assumed to be constant over the time step because the liquid interface density is considered to be a very small effect and can be neglected. Since the interface location changes with time, I_5 at time t,

$$\mathrm{I}_5(t) = \int_{z_{JST}(t)}^{z_{JEND}(t)} \rho_\ell(z)\,dz \tag{13}$$

and at t + Δt,

$$\mathrm{I}_5(t+\Delta t) = \int_{z_{JST}(t+\Delta t)}^{z_{JEND}(t+\Delta t)} \rho_\ell(z)\,dz \tag{14}$$

Taking the difference for these two variables

$$I_5(t+\Delta t) - I_5(t) = \int_{z_{JEND}(t)}^{z_{JEND}(t+\Delta t)} \rho_t(z)\, dt \; - \int_{z_{JST}(t)}^{z_{JST}(t+\Delta t)} \rho_t(z) dz \tag{15}$$

because these two integrals, Eq. (13) and Eq. (14) are identical except in segment JST and JEND, where the bubble interface positions are changing with time. The interface position z_i can be written as a linear function of the interface velocity v_i, so that

$$dz = v_i\ dt \tag{16}$$

Therefore $I_5(t + \Delta t)$ is

$$\begin{aligned} I_5(t+\Delta t) = I_5(t) &+ \rho_{ti}(JEND) \int_t^{t+\Delta t} v_i(L=1,\ t',\ K)dt' \\ &- \rho_{ti}(JST) \int_t^{t+\Delta t} v_i(L=2,\ t',\ K-1)\, dt' \end{aligned} \tag{17}$$

If the velocity is assumed vary linearly over the time step, the time integrals in (17) becomes

$$\begin{aligned} \int_t^{t+\Delta t} v_i(t')\, dt' &= \overline{v}\ \Delta t \\ &= \left(v_i(t) + \frac{\Delta v}{2} \right) \Delta t \\ &= v_i(t) \left(1 + \frac{\Delta v}{2 v_i(t)} \right) \Delta t \\ &= v_i(t) \left(1 + \frac{\Delta W}{2 W_1} \right) \Delta t \end{aligned} \tag{18}$$

where $\Delta v = v_i(t+\Delta t) - v_i(t)$. Therefore, $I_5(t + \Delta t)$ is

$$I_5(t+\Delta t) = I_5(t) + \rho_{\ell i}(JEND)\, v_i(L=1,\ t,\ k)\left(1+\frac{\Delta W}{2W_1}\right)\Delta t - \rho_{\ell i}(JST)\, v_i(L=2,\ t,\ k-1)\left(1+\frac{\Delta W}{2W_1}\right)\Delta t \tag{19}$$

Finally, Eq. (19) is rewritten as

$$I_5(t+\Delta t) = I_5(t) + \Delta I_5 + \Delta W\ I'_5 \tag{20}$$

where

$$\Delta I_5 = \Delta t\ v_i\ (L=1,\ t,\ K)\ \rho_{\ell i}(JEND)\, x_u - \Delta t\ v_i\ (L=2,\ t,\ K-1)\ \rho_{\ell i}(JST)\ x_L \tag{21}$$

$$I'_5 = \frac{\Delta I_5}{2W_1}\ , \tag{22}$$

X_L and X_U are variables which have 0.0 or 1.0 depending on liquid slug regime.

Similarly, I_1 (t + Δt) can be expressed in the same way as

$$I_1(t+\Delta t) = I_1(t) + \Delta I_1 \tag{23}$$

where

$$\Delta I_1 = \frac{\Delta t\ v_i(L=1,\ t,\ K)x_u}{A_C(JEND)} - \frac{\Delta t\ v_i(L=2,\ t,\ K-1)x_L}{A_C(JST)} \tag{24}$$

and

$$I_3(t+\Delta t) = I_3(t) + \Delta I_3 + \Delta W\ I'_3 \tag{25}$$

$$\Delta \mathrm{I}_3 = \frac{\Delta t \; v_i (L=1,\; t,\; \mathrm{K}) x_u}{2 \; \mathrm{A}_C (JEND)^2 \; \rho_{tt} (\mathrm{K}) \; D_h (JEND)} \left[\frac{D_n (JEND)}{\mathrm{A}_C (JEND) \overline{\mu} (JEND)} \right] - \frac{\Delta t \; v_i (L=2,\; t,\; \mathrm{K}-1) x_L}{2 \mathrm{A}_C (JST)^2 \; \rho_{tb} (\mathrm{K}) D_h (JST)} \left[\frac{D_h (JST)}{\mathrm{A}_C (JST) \mu (JST)} \right] \tag{26}$$

, and

$$\mathrm{I}'_3 = \frac{\Delta \mathrm{I}_3}{2W_1} \; . \tag{27}$$

Substituting the above expressions for the advanced time coefficients into Eq. (12) and neglecting second-order terms produces the differenced momentum equation

$$\begin{aligned} (I_1 + \theta_2 \Delta I_1) \frac{\Delta W}{\Delta t} &= \theta_1 (P_{b1} - P_{t1}) + \theta_2 (P_{b2} - P_{t2}) - I_2 W_1^2 \\ &- \theta_2 \Delta W W_1 I_2 - A_{fr} (I_3 + \theta_2 \Delta I_3) W_1 |W_1|^{1+b_{fr}} \\ &- (2 + b_{fr}) \theta_2 A_{fr} I_3 |W_1|^{1+b_{fr}} \Delta W - \theta_2 A_{fr} W_1 I_3' |W_1|^{1+b_{fr}} \Delta W \\ &- I_4 (W_1 |W_1| + 2\theta_2 |W_1| \Delta W) - g (I_5 + \theta_2 \Delta I_5' \theta_2 \Delta W) \end{aligned}$$

which gives

$$\Delta W = \frac{\Delta t \left| \mathrm{AA}_0 + (\Delta p_b - \Delta p_t) \theta_2 \right|}{\mathrm{I}_1 + \theta_2 \Delta \mathrm{I}_1 + \theta_2 \mathrm{BB}_0 \Delta t} \tag{28}$$

where,

$$\begin{aligned} \mathrm{AA}_0 &= p_{b1} - p_{t1} - \mathrm{I}_2 W_1^2 - \mathrm{A}_{fr} (\mathrm{I}_3 + \theta_2 \Delta \mathrm{I}_3) W_1 |W_1|^{1+b_{fr}} \\ &\quad - \mathrm{I}_4 W_1 |W_1| - g (\mathrm{I}_5 + \theta_2 \Delta \mathrm{I}_5) \end{aligned}$$

$$\begin{aligned} \mathrm{BB}_0 &= 2 \; W_1 \; \mathrm{I}_2 + (2 + b_{fr}) \mathrm{A}_{fr} \mathrm{I}_3 |W_1| 1 + b_{fr} + 2 \mathrm{I}_4 |W_1| \\ &\quad + \mathrm{A}_{fr} |W_1| 1 + b_{fr} \; W_1 \mathrm{I}_3' + g \mathrm{I}_5' \end{aligned}$$

Thus, the change in flow rate for a liquid slug is related to the changes in vapor pressures in the bubbles above and below the liquid slug, or to the changes in inlet and outlet coolant pressures.

3. Interfave velocities

The average velocity in a liquid slug is

$$v_\ell = \frac{W}{\rho_\ell A_C} \tag{29}$$

If the coolant channel volume between $Z_i(t)$와 $Z_i(t + \Delta t)$ is taken as a control volume in Fig. 2, then the liquid volume in the control volume at time t is

$$V_\ell(t) = P_e\, v_i \Delta t \left(W_{fe} + r_2\, W_{fs}\right) \tag{30}$$

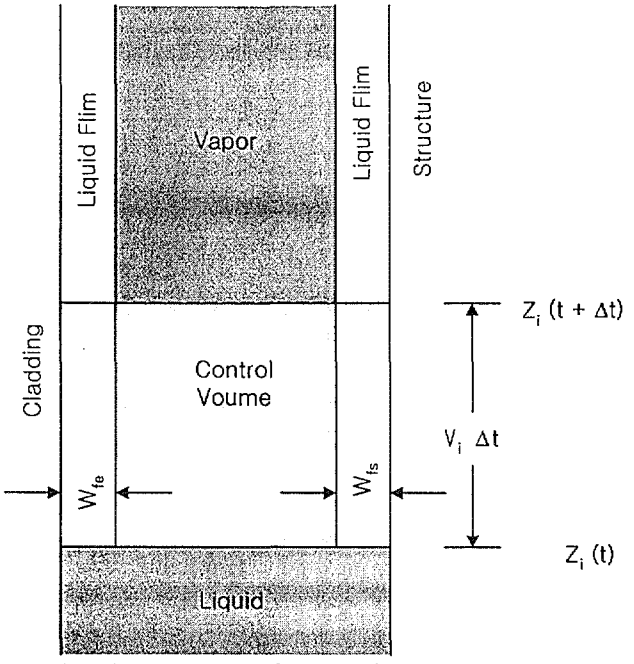

Fig. 2 Control Volume for Interfacial Velocity Calculation

where P_e ≒ is the outer perimeter of the cladding and γ_2 ≒ is the ratio of the surface area of the structure to the surface area of the cladding. At t + Δt, the liquid volume in the control volume is

$$V_\ell\,(t+\Delta t) \;=\; A_C\; v_i\,\Delta t \tag{31}$$

Accounting for the liquid added to and subtracted from the control volume during Δt gives

$$V_\ell\,(t+\Delta t) = V_\ell\,(t) + v_\ell A_C \Delta t - P_e\,\left(W_{fe}\;V_{fe}\;+\;r_2 W_{fs} V_{fs}\right)\Delta t \tag{32}$$

Substituting Eq. (30) and (31) into (32) gives

$$\begin{aligned} A_C\,v_i\,\Delta t \;&=\; P_e v_i \Delta t\left(W_{fe}\;+\;r_2\,W_{fs}\right) + v_\ell\,A_C\,\Delta t \\ &\quad - P_e \Delta t\left(W_{fe}\,v_{fe}\;+\;r_2\,W_{fs}\,v_{fs}\right) \end{aligned} \tag{33}$$

or

$$v_i \;=\; \frac{v_\ell - p_e\left(W_{fe}\,v_{fe}\;+\;r_2\,W_{fs}\,v_{fs}\right)/\,A_C}{1 - p_e\left(W_{fe}\;+\;r_2\;W_{fs}\right)/\,A_C} \tag{34}$$

4. Bubble Formation and Collapse

4.1 Basic Assumptions for Vapor Bubble Modeling

Vapor is assumed to be formed if user-specified amount of superheat is satisfied at a node. If the user-specified amount of superheat is exceeded in a node, then time-step size is reduced, and coolant calculations for channel are repeated for the time step, so as to satisfy the superheat criterion exactly at the end of time step. A similar test is made at the end of each coolant time step for formation of new bubbles after the voiding has started. This model, however, is subjected to the following limitations.

(i) If new bubbles are formed in a channel, the maximum of 9 bubbles are allowed ;

(ii) No new bubbles will be formed within a minimum distance adjacent to a bubble-liquid interface, and, thus, nodes within the distance of the interface are not examined for bubble formation ;

(iii) No more than one bubble will be formed within a time-step

(iv) When the superheat criterion is exceeded, a new bubble is formed with whatever superheat happens to exist.

Bubbles are assumed to fill the whole cross section of the coolant channel, except for a liquid film left on the cladding and structure as shown in Fig. 3. The vapor growing attributes mainly to vaporization of the liquid film on the cladding.

For small bubbles the pressures are uniform spatially inside the bubbles, whereas there exists pressure gradient for a bubble length exceeding the specified minimum size(5～10 cm). Thus, different model must be applied because axial distribution of the pressure cannot be ignored. The shrink of a vapor bubble is possible because of condensation in the cooler region. The vapor length and the decreasing rate of the size is simultaneously below the minimum value, the vapor disappears. Two liquid slugs are then combined into one.

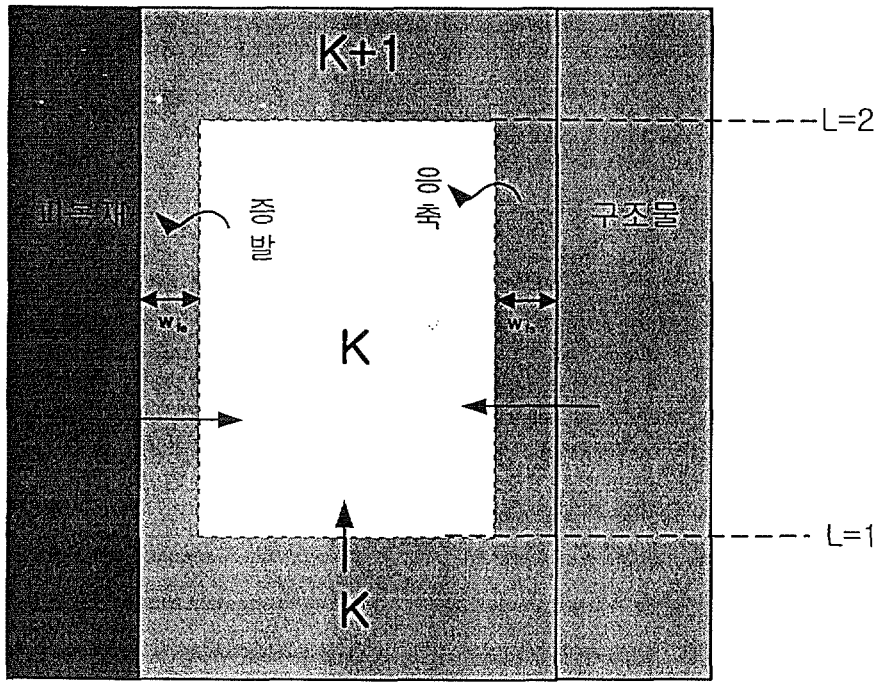

Fig. 3 Uniform Vapor Pressure Bubble Model

The present SOBOIL model has been developing based on the uniform pressure model which is adequate to small bubbles. The bubble growth is determined by coupling the momentum equations for the liquid slugs, as described in Section 2, with an energy balance in the vapor bubble, assuming saturation conditions and spatially uniform pressure and temperature within a bubble. The rate of formation and condensation of vapor is determined by the heat flow through the liquid films on the cladding and structure and through the liquid-vapor interfaces. Fig. 3 shows the control volume considered in the uniform vapor pressure model. The control volume extends from the lower liquid-vapor interface to the upper one, and from the outer surface of the cladding to the inner surface of the structure. This means that the liquid film remaining on the structure and cladding is included in the control volume. The primary focus of this model is to obtain the temperature within the vapor bubble. Once temperature is known, it can be used to calculate the vapor pressure, since saturation conditions have been assumed. The vapor pressure is the driving force for motion of the liquid slugs, so finding the vapor pressures in all bubbles provides the link between conditions in the liquid slugs and conditions in the bubbles and therefore leads to a complete description of conditions throughout the channel.

The vapor temperature is found by taking an energy balance within the control volume described above. The energy balance can be stated qualitatively as

Net energy transferred to the volume =
Net change in energy within the volume

The energy transferred to the control volume can be divided into two sources:

Energy transferred = (Heat flow from the cladding and the structure)
+ (Heat flow through the vapor-liquid interfaces)

Changes in energy = (Energy change due to temperature change of vapor
Present at time t) + (Energy change due to
Vaporization or condensation during the time step)

The reminder of this section will formulate equations that model each portion of the energy balance and that, when combined, will reduce to a set of linear equations that give the vapor temperatures of the bubbles in the channel in terms of known quantities.

4.2 Description of the uniform pressure bubble

The total energy added to vapor bubble K in a time step is

$$E_t = \int_t^{t+\Delta t} \tilde{Q}(\tau)\, d\tau \tag{35}$$

where Q is the total heat energy flow rate into the vapor:

$$\tilde{Q} = \int_s q \; ds, \tag{36}$$

q is the surface heat flux, and s is the vapor surface. The total heat energy is the sum of the energy flow from the cladding and structure, Ees, and the energy flow through the liquid-vapor interfaces, Ei :

$$E_t = E_{es} + E_i. \tag{37}$$

The cladding and structure term, Ees, is approximated by

$$E_{es} = \frac{\Delta t}{2}\left[Q_{es}(k,t) + Q_{es}(k,t+\Delta t)\right] \tag{38}$$

where Q_{es} is the heat flow from the cladding and structure,

$$Q_{es}(k,t) = P_e \int_{Z_i(L=1,t,K)}^{Z_i(L=2,t,K)} \left[q_e(z,t) + \gamma_2 q_s(z,t)\right] dz \tag{39}$$

with

$Z_i(2,t,K)$ = height of upper liquid-vapor interface

$Z_i(1,t,K)$ = height of lower liquid-vapor interface

P_e = perimeter of cladding = $2\pi r_e$

r_e = nominal radius of cladding

γ_e = rate of surface area of structure to surface area of cladding

q_e = cladding-to-vapor heat flux

and

q_s = structure-to-vapor heat flux

The heat fluxes are calculated as

$$q_e(z,t) = \frac{T_e(z,t) - T(k,t)}{R_{ec}(z,t)} \tag{40}$$

and

$$q_s(z,t) = \frac{T_s(z,t) - T(k,t)}{R_{sc}(z,t)} \tag{41}$$

where T(K,t) is the uniform temperature within bubble K at time t and R_{ec} and R_{sc} are the thermal resistances between the cladding and vapor and the structure and vapor, respectively. The total thermal resistance is then the sum of the individual resistance, or

$$R_{ec} = \frac{1}{h_{ec}} + R_{ehf} \tag{42}$$

where R_{ehf} is the resistance of the cladding and h_{ec} is the heat transfer coefficient which models the combined resistances of the liquid film and the vapor. The coeficient hec is just $1/(\frac{1}{h_c} + \frac{w_{fe}}{k_t})$; however, this is not as simple an expression as it appears, since the convective heat-transfer coefficient h_c is not a constant or a simple function of temperature. To circumvent this difficulty, h_{ec} for a temperature correlation based on physical data used in SAS2A is used. The coefficient h_{ec} then takes the form

$$h_{ec}(z)=\frac{k_\ell(z)}{w_{fe}(z)} \qquad if\ T_e(z) > T(k) + 100 \tag{43}$$

where

$k_\ell(z)$ = thermal conductivity of liquid sodium at temperature T(K)

and

$w_{fe}(z)$ = thickness of liquid film on the cladding

and T(K) represents an extrapolated vapor temperature for advanced time values of h_{ec}. If the cladding is more than 100 K colder than the vapor, the liquid film is assumed to be at the same temperature as the cladding, and so the resistance of the film is neglected. The heat-transfer coefficient from the vapor to the film is a condensation coefficient h_{cond} which is currently given as 6 x 10^4 W/m^2-K. The coefficient h_{ec} then becomes

$$h_{ec}(z)=h_{cond} \qquad if\ T_e(z) < T(k) - 100 \tag{44}$$

and

$$h_{ec}(z)=h_{cond}+\frac{\frac{k_\ell(z)}{w_{fe}(z)}-h_{cond}}{1+\exp\left(\frac{T(k)-T_e(z)}{2}\right)}, \qquad T(k)-100<T_e(z)<T(k)100 \tag{45}$$

The thermal resistance between the structure and the vapor is calculated using the same procedure as for the cladding. The thermal resistance is defined as

$$R_{sc}=\frac{1}{h_{sc}}+\frac{d_{sti}}{2k_{sti}} \tag{46}$$

with the structure thermal resistance defined as the ratio of d_{sti}, the thickness of the inner structure node, to twice the structure thermal conductivity k_{sti}, and the heat-transfer coefficient h_{sc}

$$h_{sc}(z)=\frac{k_\ell(z)}{w_{fs}(z)} \qquad if\ T_s(z) > T(k) + 100 \tag{47}$$

$$h_{sc}(z) = h_{cond} \qquad if\ T_s(z) < T(K) - 100 \tag{48}$$

and

$$h_{sc}(z) = h_{cond} + \frac{\frac{k_\ell(z)}{w_{fs}(z)} - h_{cond}}{1 + \exp\frac{T(k) - T_s(z)}{2}}, T(k) - 100 < T_s(z) < T(k) + 100 \tag{49}$$

With the cladding-to-vapor and structure-to-vapor heat fluxes now defined, Eq. (39) can be solved for $Q_{es}(K,t)$ in terms of known quantities. The problem now is to use Eq. (39) to express $Q_{es}(K, \Delta t)$ as a linear function of the change in vapor temperatures over the time step Δt. The difficulty comes from that the advanced time interface positions z_i (which are the limits of integration in the expression for $Q_{es}(K, \Delta t)$) are dependent on the advanced time vapor pressures and, therefore, on the advanced time temperature changes if the interface positions are written as the sum of two functions, one which contains only known quantities and one which is a linear function of the change in vapor temperature. To this end, interface position at $t + \Delta t$ can be written as a linear function

$$z_i(L, t + \Delta t, k) = z_i(L, t, k) + \Delta z_i(k, L) \tag{50}$$

with the change in position Δz_i given by

$$\Delta z_i(K, L) = \frac{\Delta t}{2}\left(v_i(L, t, k) + v_i(L, t + \Delta t, K)\right). \tag{51}$$

The advanced time interface velocity can also be expressed as a linear function

$$v_i(L,t+\Delta t,K)=v_i(L,t,K)+\Delta v_i(K,L) \tag{52}$$

with the change in interface velocity computed from the change in liquid slug mass flow rate

$$\Delta v_i(K,L)=\frac{\Delta w(K')}{(\rho_\ell A_c)_{K',L}} \tag{53}$$

where

$$K' = K \qquad if\ L=1,$$

$$K' = K+1 \qquad if\ L=2,$$

and $(\rho_\ell A_c)_{k',L}$ is a product of the liquid density and channel flow area at the bubble interface. It is assumed in Eq. (53) that the change in interface velocity can be expressed as the change in the average slug velocity, with the correction for film thickness ignored. If now the expression for the change in liquid slug mass flow rate, Eq. (28), is combined with Eq. (53) and inserted into Eq. (52), the advanced time interface velocity becomes

$$v_i(L,t+\Delta t,K)=v_i(L,t,K)+\frac{1}{(\rho_\ell A_c)_{K',L}}\frac{\Delta t\left[AA_0(K')+(\Delta p_{K'-1}-\Delta p_{K'})\theta_2\right]}{I_1(K')+\theta_2\ \Delta I_1(K')+\theta_2 BB_0(K')\Delta t} \tag{54}$$

with

$$\begin{aligned} z_i(L,t+\Delta t,K) &= z_i(L,t,K)+v_i(L,t,K)\ \Delta t \\ &+\frac{\Delta t}{2}\frac{1}{(\rho_\ell A_c)_{K',L}}\frac{\Delta t\left[AA_0(K')+(\Delta p_{K'-1}-\Delta p_{K'})\theta_2\right]}{I_1(K')+\theta_2\ \Delta I_1(K')+\theta_2 BB_0(K')\Delta t} \end{aligned} \tag{55}$$

which can be rewritten as

$$z_i(L,t+\Delta t,K) = z_{i0}(K,L)+\Delta z'(K,L) \tag{56}$$

where z_{i0}(K, L) is the function

$$z_{i0}(K,L) = z_i(L,t,K) + \Delta z_0(K,L) \tag{57}$$

with

$$\Delta z_0(K,\ L) = v_i(L,t,K)\Delta t + \frac{1}{2}\frac{\Delta w_0(K')\Delta t}{(\rho_t A_c)_{K',L}} \tag{58}$$

and

$$\Delta w_0(K') = \frac{AA_0(K')\Delta t}{I_1(K') + \theta_2\ \Delta I_1(K') + BB_0(K')\theta_2\,\Delta t} \tag{59}$$

and $\Delta z'$(K, L) is

$$\Delta z'(K,L) = \frac{dz_i(K,L)}{dp}\left(\Delta p_{K'-1} - \Delta p_{K'}\right) \tag{60}$$

with

$$\frac{dz_i(K,L)}{dp} = \frac{\theta_2\,\Delta t^2}{2(\rho_t A_c)_{K',L}\left[I_1(K') + \theta_2\,\Delta I_1(K') + BB_0(K')\theta_2\Delta t\right]} \tag{61}$$

The expression for $\frac{dz_i}{dp}$ is obtained by taking the derivative with respect to pressure of Eq. (51), using Eq.(54). The function z_{i0}(K, L) is a function only of known quantities and is the approximate position to which the interface would move at t+Δt if the bubble pressures did not change over the time step. The additional change in interface position due to bubble pressure changes is accounted for by $\Delta z'$, which is a linear function of the pressure changes.

Using Eq.(57) for the interface position, the integral for the cladding and structure heat

flow $Q_{es}(K, t+\Delta t)$ can be expressed as the sum of three integrals :

$$Q_{es}(K,t+\Delta t) = P_e \int_{z_{i0}(k,1)}^{z_{i0}(k,2)} \left[q_e(z,t+\Delta t)+\gamma_2 q_s(z,t+\Delta t)\right] dz$$
$$+ P_e \int_{z_{i0}(K,2)}^{z_{i0}(K,2)+\Delta z'(K,2)} \left[q_e(z,\ t+\Delta t)+\gamma_2 q_s(z,\ t+\Delta t)\right] dz \qquad (62)$$
$$+ P_e \int_{z_{i0}(K,1)+\Delta z'(K,1)}^{z_{i0}(K,1)} \left[q_e(z,\ t+\Delta t)+\gamma_2 q_s(z,\ t+\Delta t)\right] dz$$

If the vapor temperature T(K, t+Δt) is linearized to be T(K, t) + ΔT(K), the first integral is a function only of ΔT(K) and known quantities, since the advanced time cladding and structure temperatures are determined by extrapolation from values calculated in the transient heat-transfer module at the previous two heat-transfer time steps and, therefore, are considered known. Using Eq.(40) and (41) for the heat fluxes, the first integral can be written as the sum $I_{e1}(K) + I_{e2}(K)\Delta T$, where

$$I_{e1}(K) = P_e \int_{z_{i0}(K,1)}^{z_{i0}(K,2)} \left\{ \frac{T_e(z,\ t+\Delta t)-T(K,t)}{R_{ec}(z,\ t+\Delta t)} + \frac{\gamma_2\left[T_s(z,\ t+\Delta t)-T(K,\ t)\right]}{R_{sc}(z,\ t+\Delta t)} \right\} dz \qquad (63)$$

and

$$I_{e2}(K) = -P_e \int_{z_{i0}(K,1)}^{z_{i0}(K,2)} \left\{ \frac{1}{R_{ec}(z,\ t+\Delta t)} + \frac{\gamma_2}{R_{sc}(z,\ t+\Delta t)} \right\} dz \qquad (64)$$

The second and third integrals are evaluated by assuming that the heat fluxes are constant in space over the domain of integration; This is reasonable assumption, since Δz' is a small quantity. If second-order terms proportional to ΔTΔz' are dropped, the second integral is just $I_{e3}(K)\Delta z'(K, 2)$, with

$$I_{e3}(K)=P_e\left\{\frac{T_e\left[z_{i0}(K,\ 2),\ t+\Delta t\right]-T(K,\ t)}{R_{ec}\left[z_{i0}(K,\ 2),\ t+\Delta t\right]}+\gamma_2\left[\frac{T_s\left[z_{i0}(K,\ 2),\ t+\Delta t\right]-T(K,\ t)}{R_{sc}\left[z_{i0}(K,\ 2),\ t+\Delta t\right]}\right]\right\} \tag{65}$$

and the third integral is $I_{e4}(K)\Delta z'(K, 1)$, where

$$I_{e4}(K)=P_e\left\{\frac{T_e\left[z_{i0}(K,\ 1),\ t+\Delta t\right]-T(K,\ t)}{R_{ec}\left[z_{i0}(K,\ 1),\ t+\Delta t\right]}+\gamma_2\left[\frac{T_s\left[z_{i0}(K,\ 1),\ t+\Delta t\right]-T(K,\ t)}{R_{sc}\left[z_{i0}(K,\ 1),\ t+\Delta t\right]}\right]\right\} \tag{66}$$

This gives for $Q_{es}(K, t+\Delta t)$

$$Q_{es}(K,\ t+\Delta t)\ =\ I_{e1}(K)\ +\ I_{e2}(K)\Delta T(K)+I_{e3}(K)\Delta z'(K,\ 2)+I_{e4}(K)\Delta z'(K,\ 1) \tag{67}$$

which, by the definition of $\Delta z'$ and the assumption of saturation conditions, is a function only of known quantities and the changes in bubble temperatures.

The energy flow in Ees is therefore given by the linear equation

$$E_{es}=\frac{\Delta t}{2}\left[Q_{es}(K,\ t)+I_{e1}(K)+\left(I_{e2}(K)+I_{e3}(K)\frac{dz_i\ (K,\ 2)}{dp}-I_{e4}(K)\frac{dz_i\ (K,\ 1)}{dp}\right)\Delta p_K-I_{e3}(K)\frac{dz_i\ (K,\ 1)}{dp}\Delta p_{K+1}+I_{e4}(K)\frac{dz_i\ (K,\ 1)}{dp}\Delta p_{K-1}\right] \tag{68}$$

where the definition of $\Delta z'$ in terms of ΔP has been used.

4.3 Heat Conduction Equation

The one-dimensional heat conduction equations are set up in order to calculate temperature distribution within the fuel and structure with given boundary conditions in a cylindrical coordinate. The numerical method is applied to solving the equation because analytical method is not suitable to solve the equation for complex geometry and physical properties of the solid with the non-uniform heat generation rate. This model is developed primarily with a semi-implicit method, however, fully implicit method is also available if necessary. The maximum 50 nodes are currently allowed for solving the equations.

4.3.1 Governing Equation

A general form of the conduction equation is given by

$$\rho c \frac{\partial T}{\partial t} = k \nabla^2 T + q''' \tag{69}$$

The above equation is rewritten for one dimensional problem as

$$\rho c \frac{\partial T}{\partial t} = k \frac{d^2 T}{dx^2} + q''' \tag{70}$$

4.3.2 Inner Nodes

Integrating Eq. (70) over the node volumes and differentiate it from node j to node l, the resulting equation is given through some arrangement by Eq. (71).

$$\rho c \int_V \frac{\partial T}{\partial t} dV = \int_V \frac{\partial}{\partial x}\left(k \frac{\partial T}{\partial x}\right) dV + \int_V q''' dV$$

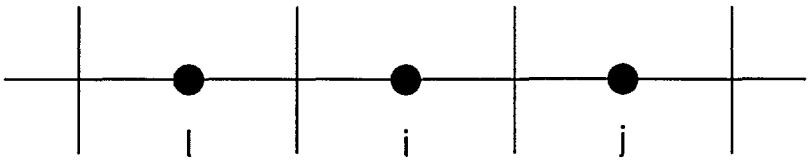

Fig. 4 Control Volume for Heat Conduction Equation

$$\rho c \int_l^j \frac{\partial T}{\partial t} dx\Delta y\Delta z = \int_l^j \frac{\partial}{\partial x}(k\frac{\partial T}{\partial x}) dx\Delta y\Delta z + \int_v q''' dx\Delta y\Delta z$$

$$\rho c \frac{\partial T}{\partial t} \Delta x\Delta y\Delta z = \left[k\frac{\partial T}{\partial x} \Delta y\Delta z \right]_l^j + q''' \Delta x\Delta y\Delta z$$

where, since $\Delta x\Delta y\Delta z = V$ and $\Delta y\Delta z = A$,

$$\rho c \frac{\partial T}{\partial t} V = \left[k\frac{\partial T}{\partial x} A \right]_l^j + q''' V$$

$$\rho_i c_i \frac{\partial T_i}{\partial t} V_i = \left[\frac{k_{ij}(T_i - T_j) A_{ij}}{d_{ij}} + \frac{k_{il}(T_i - T_l) A_{il}}{d_{il}} \right] + q''' V_i$$

$$\rho_i c_i V_i \frac{\partial T_i}{\partial t} + \left[-\frac{k_{ij} A_{ij}}{d_{ij}} T_j - \frac{k_{il} A_{il}}{d_{il}} T_l + \left(\frac{k_{ij} A_{ij}}{d_{ij}} + \frac{k_{il} A_{il}}{d_{il}} \right) T_i \right] = q_i^{\cdot} V_i \qquad (71)$$

The Eq. (2.71) is, then, defined in the following way to express in the matrix form

$$\rho_i c_i V_i = cmat(i) \qquad (72)$$

$$-\frac{k_{ij} A_{ij}}{d_{ij}} T_j = smat3(i) \qquad (73)$$

$$-\frac{k_{il}\,A_{il}}{d_{il}}T_l = smat1(i) \tag{74}$$

$$\frac{k_{ij}\,A_{ij}}{d_{ij}} + \frac{k_{il}\,A_{il}}{d_{il}} = smat2(i) \tag{75}$$

$$\bar{q_i} = rmat(i) \tag{76}$$

$$cmat(i)\frac{dT_i}{dt} + [\,smat3(i)T_j + smat1(i)T_l + smat2(i)T_i\,] \;=\; rmat(i) \tag{77}$$

where $\frac{dT_i}{dt}$ can be expressed as $\frac{T_i^{n+1} - T_i^n}{\Delta t}$, and T j, T l, and Ti are done depending on a numerical scheme, i.e. Explicit scheme, Crank-Nicolson scheme, Fully-implicit scheme. When the Crank-Nicolson scheme which defines T with the average of the previous time step and the advanced time step values, is applied to Eq. (77), and arrange it, then, the Eq. (2.77) can be rewritten as

$$\begin{aligned} cmat(i)\frac{T_i^{n+1} - T_i^n}{\Delta t} + [\,smat3(i)(\frac{T_j^{n+1} + T_j^n}{2}) \\ + smat1(i)(\frac{T_l^{n+1} + T_l^n}{2}) + smat2(i)(\frac{T_i^{n+1} + T_i^n}{2})\,] \;=\; rmat(i) \end{aligned} \tag{78}$$

The form, now, looks like

$$C \bullet T_1 \;+\; S \bullet T_2 \;=\; R \tag{79}$$

where

$$C = \begin{pmatrix} \frac{cmat(1)}{\Delta t} & 0 & .... & 0 \\ 0 & \frac{cmat(2)}{\Delta t} & 0 & 0 \\ 0 & 0 & .... & 0 \\ 0 & .... & 0 & \frac{cmat(N)}{\Delta t} \end{pmatrix}$$

$$S = \begin{pmatrix} smat2(1) & smat1(1) & 0 & 0 & .... & 0 \\ smat3(2) & smat2(2) & smat1(2) & 0 & .... & 0 \\ 0 & smat3(3) & smat2(3) & smat1(3) & .... & 0 \\ 0 & 0 & smat3(4) & smat2(4) & smat1(4) & 0 \\ .... & .... & .... & .... & .... & .... \\ 0 & 0 & 0 & .... & smat3(N) & smat2(N) \end{pmatrix}$$

$$T_1 = \begin{pmatrix} T(1)^{n+1} - T(1)^n \\ T(2)^{n+1} - T(2)^n \\ .... \\ T(N)^{n+1} - T(N)^n \end{pmatrix}$$

$$T_2 = \begin{pmatrix} \frac{T(1)^{n+1} - T(1)^n}{2} \\ \frac{T(2)^{n+1} - T(2)^n}{2} \\ .... \\ \frac{T(N)^{n+1} - T(N)^n}{2} \end{pmatrix}$$

$$R = \begin{pmatrix} rmat(1) \\ rmat(2) \\ .... \\ rmat(N) \end{pmatrix}$$

The advanced time step, n+1 time step values are unknown and n time step values are known

as the previous time step. Terms involving unknown variables are placed in the left hand side of the equation and it becomes

$$C^{'} \bullet T^{n+1} \;=\; S^{'} \bullet T^{n} \;+\; R \tag{80}$$

where

$C^{'} \;=$

$$\begin{pmatrix}
\frac{cmat(1)}{\Delta t}+\frac{smat2(1)}{2} & \frac{smat1(1)}{2} & 0 & 0 & .... & 0 \\
\frac{smat3(2)}{2} & \frac{cmat(2)}{\Delta t}+\frac{smat2(2)}{2} & \frac{smat1(2)}{2} & 0 & .... & 0 \\
0 & \frac{smat3(3)}{2} & .... & .... & .... & 0 \\
0 & .... & .... & .... & .... & 0 \\
0 & .... & .... & .... & .... & 0 \\
0 & 0 & 0 & .... & \frac{smat3(N)}{2} & \frac{cmat(N)}{\Delta t}+\frac{smat2(N)}{2}
\end{pmatrix} \tag{2.81}$$

$S^{'} \;=$

$$\begin{pmatrix}
\frac{cmat(1)}{\Delta t}-\frac{smat2(1)}{2} & -\frac{smat1(1)}{2} & 0 & 0 & .... & 0 \\
-\frac{smat3(2)}{2} & \frac{cmat(2)}{\Delta t}-\frac{smat2(2)}{2} & -\frac{smat1(2)}{2} & 0 & .... & 0 \\
0 & \frac{smat3(3)}{2} & .... & .... & .... & 0 \\
0 & .... & .... & .... & .... & 0 \\
0 & .... & .... & .... & .... & 0 \\
0 & 0 & 0 & .... & -\frac{smat3(N)}{2} & \frac{cmat(N)}{\Delta t}-\frac{smat2(N)}{2}
\end{pmatrix} \tag{2.82}$$

$$T^{n+1} = \begin{pmatrix} T(1)^{n+1} \\ T(2)^{n+1} \\ .... \\ T(N)^{n+1} \end{pmatrix} \tag{83}$$

$$T^{n} = \begin{pmatrix} T(1)^{n} \\ T(2)^{n} \\ .... \\ T(N)^{n} \end{pmatrix} \tag{84}$$

Therefore, the transient temperature distribution can be solved once the initial temperatures are known. For the fully implicit method, the equation of the matrix form is same as Eq. (80) except S' matrix elements.

4.3.3 Boundary Conditions

The present model allows four boundary conditions, i.e. specified heat flux, convection, adiabatic, and specified temperature.

(1) Specified Heat Flux

The energy conservation equation for a given heat flux at wall surface can be written as

$$q_{ji} + q_i^{"} S_i + \dot{E}_{gi} = \dot{E}_{si} \tag{85}$$

By differentiating Eq. (85), it becomes

$$\frac{k_{ij} A_{ij}}{d_{ij}} (T_j - T_i) + q_i^{"} S_i + q^{"'} V_i = \rho_i c_i V_i \frac{dT_i}{dt} \tag{86}$$

It can further be rearranged for a convenience as

$$\rho_i c_i V_i \frac{\partial T_i}{\partial t} + \left[-\frac{k_{ij} A_{ij}}{d_{ij}} T_j + \frac{k_{ij} A_{ij}}{d_{ij}} T_i \right] = \bar{q_i} V_i + \dot{q_i} S_i \tag{87}$$

Eq. (87) is applied to the node 1 and then it is numerically differentiated using Crank-Nicolson scheme

$$\begin{aligned} &\frac{cmat(1)}{\Delta t} T(1)^{n+1} + \frac{smat3(1)}{2} T(2)^{n+1} + \frac{smat2(1)}{2} T(1)^{n+1} \\ &= \frac{cmat(1)}{\Delta t} T(1)^{n} - \frac{smat3(1)}{2} T(2)^{n} - \frac{smat2(1)}{2} T(1)^{n} + rmat(1) \end{aligned} \tag{88}$$

where smat2(1) and rmat(1) are redefined as

$$smat2(1) = \frac{k_{ij} A_{ij}}{d_{ij}} \tag{89}$$

$$rmat(1) = \dot{q_i} S_i + \bar{q} V_i \tag{90}$$

(2) Convection

This boundary condition is applied to the condition where the wall surface is cooled down or heated up with the heat transfer coefficient, h. The energy conservation equation for a heat transfer coefficient at wall surface can be written as

$$q_{ji} + q_{conv,i} + \dot{E}_{gi} = \dot{E}_{si} \tag{91}$$

By differentiating Eq. (91), it becomes

$$\frac{k_{ij} A_{ij}}{d_{ij}} (T_j - T_i) + h_i S_i (T_{bi} - T_i) + \bar{q} V_i = \rho_i c_i V_i \frac{dT_i}{dt} \tag{92}$$

It can further be rearranged for a convenience as

$$\rho_i c_i V_i \frac{\partial T_i}{\partial t} + \left[-\frac{k_{ij} A_{ij}}{d_{ij}} T_j + \left(\frac{k_{ij} A_{ij}}{d_{ij}} + h_i S_i \right) T_i \right] = q_i^{"} V_i + q_i^{'} S_i \quad (93)$$

In the matrix form smat2(1) and rmat(1) are redefined as

$$smat2(1) = \frac{k_{ij} A_{ij}}{d_{ij}} + h_i S_i \quad (94)$$

$$rmat(1) = h_i S_i T_{bi} + q^{"} V_i \quad (95)$$

(3) The same equation as that used for the specified heat flux and $q_i^{"} = 0$.

(4) Specified Temperature

The difference equation for the node near the boundary (i.e. node 2 or node N-1) is given as

$$\rho_i c_i V_i \frac{dT_i}{dt} + \left[-\frac{k_{ij} A_{ij}}{d_{ij}} T_j - \frac{k_{il} A_{il}}{d_{il}} T_l + \left(\frac{k_{ij} A_{ij}}{d_{ij}} + \frac{k_{il} A_{il}}{d_{il}} \right) T_i \right] = q^{"} V_i \quad (96)$$

Since the boundary temperature, Ti, is known, the term including Tl is considered as a source term.

$$\rho_i c_i V_i \frac{dT_i}{dt} + \left[-\frac{k_{ij} A_{ij}}{d_{ij}} T_j + \left(\frac{k_{ij} A_{ij}}{d_{ij}} + \frac{k_{il} A_{il}}{d_{il}} \right) T_i \right] = \frac{k_{il} A_{il}}{d_{il}} T_l + q^{"} V_i \quad (97)$$

Eq. (97) is applied to the node 2 and then it is numerically differentiated using Crank-Nicolson scheme

$$\frac{cmat(2)}{\Delta t}T(2)^{n+1} + \frac{smat3(2)}{2}T(3)^{n+1} + \frac{smat2(2)}{2}T(2)^{n+1} = \frac{cmat(2)}{\Delta t}T(2)^{n} - \frac{smat3(2)}{2}T(3)^{n} - \frac{smat2(2)}{2}T(2)^{n} + rmat(2) \tag{98}$$

where smat2(1) and rmat(1) are redefined as

$$smat2(2) = \frac{k_{ij}A_{ij}}{d_{ij}} + \frac{k_{il}A_{il}}{d_{il}} \tag{99}$$

$$rmat(2) = \frac{k_{il}A_{il}}{d_{il}}T_l + \bar{q}V_i \tag{100}$$

4.3.4 Stability

The following form of equation is obtained by differentiating the conduction equation numerically.

$$a_iT_i = a_j[fT_j + (1-f)T_j^0] + a_l[fT_l + (1-f)T_l^0 + [a_i^0 - (1-f)a_i - (1-f)a_l]T_i^0 \tag{101}$$

where the superscript 0 indicates the previous values and a_i, a_i^0, a_j, a_l are defined as follows :

$$a_i^0 = \frac{\rho_i c_i V_i}{\Delta t} \tag{102}$$

$$a_j = \frac{k_{ij}A_{ij}}{d_{ij}} \tag{103}$$

$$a_l = \frac{k_{il}A_{il}}{d_{il}} \tag{104}$$

$$a_i = f a_j + f a_l + a_i^0 \tag{105}$$

Since T_i must increase as T_i^0 rises, the coefficients of Ti and T_i^0 must have the same signs for stable solutions all the time. It will show oscillatory behavior if they are different each other.

(1) Explicit Scheme

For explicit scheme, f = 0 in Eq. (101) and thus a_i is always positive. The coefficient of T_i^0 must be positive for stable solutions, i.e.

$$a_i^0 - a_j - a_l > 0 \tag{106}$$

Definitions of those values in Eq. (102) through (104) are introduced in Eq. (106) and then the following stable condition is obtained.

$$\Delta t < \frac{\rho_i c_i (d_{ij} d_{il})}{2k} \tag{107}$$

(2) Semi-implicit Scheme (Crank-Nicolson Scheme)

For Crank-Nilconson Scheme, f = 0.5 and the same procedure is applied to Eq. (101) and the following stable condition is obtained.

$$\Delta t < \frac{\rho_i c_i (d_{ij} d_{il})}{k} \tag{108}$$

As an example, the developed model is applied to the Inconel pipe (inner diameter = 0.0169164 m, outer diameter = 0.01905 m) with the initial condition of 600 K and inner and outer surfaces are kept temperatures of 800 K and 600 K, respectively. The conductivity for

the Inconel is given as k = 17.71 W/(m-K) and ρC_p = 4.35 x 10^6 J/(m^3 – K). If it is modeled with 3 nodes, the maximum time step is estimated Δt = 0.035 sec. The following figures 5, 6 are calculated results for time step of Δt = 0.1 sec and stable time step at the inner node from the outer boundary.

As shown in the results, the temperature with the time step larger than the stable time step oscillates but it converges ultimately. (Fig. 5) The stable solution, however, is obtained without oscillation for the stable time step. (Fig. 6) Figure 7 summerizes the temperature response to the time step and as time step increases, it approaches the linear profile.

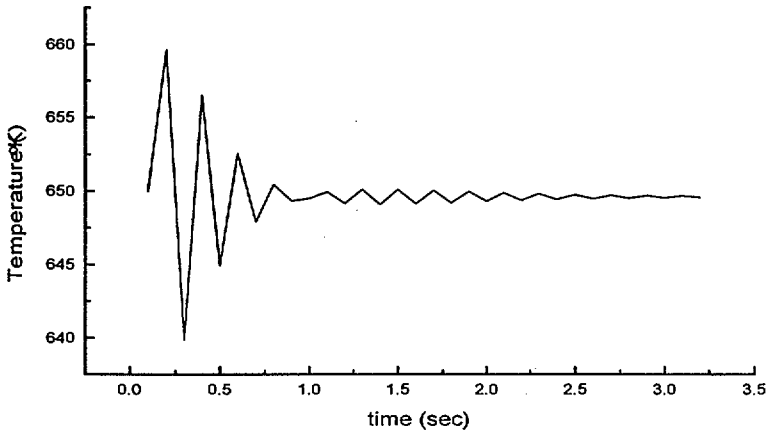

Δt = 0.1 (sec)

Fig. 5 Temperature response with the time-step larger than the stable time step

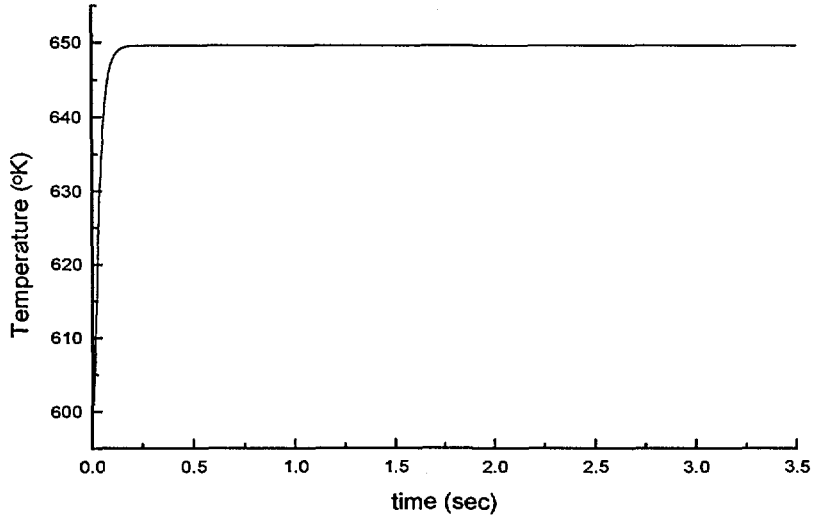

Fig. 6 Temperature response with the stable time step

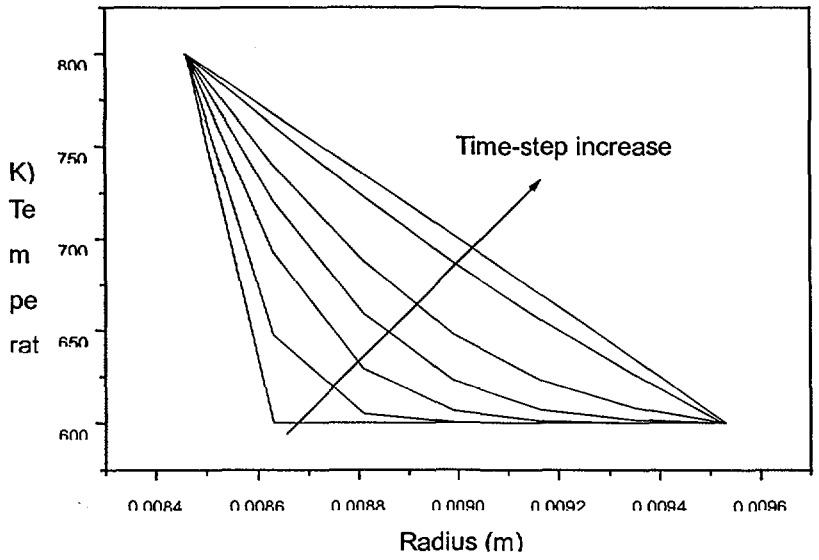

Fig. 7 Temperature response to the time step

5. Interface Temperature

The interface between a vapor and a liquid slug moves along the axis, Eulerian calculation is not considered to be proper. The basic equation for liquid temperature can be rewritten as

$$\rho c \frac{dT_c}{dt} = \gamma\varphi(z,t) + Q_c(z,t) \tag{109}$$

where the Lagrangian total time derivative dT_c/dt, as seen by an observer moving with the coolant velocity, is used. This derivative is approximated by

$$\frac{dT_c}{dt} = \frac{T_c(z,t+\Delta t) - T_c(z-\Delta z,t)}{\Delta t} \tag{110}$$

where

$$\Delta z = \frac{[G(t+\Delta t)+G(t)]\Delta t}{2\bar{\rho}(z)} \tag{111}$$

The Lagrangian calculation is used to calculate liquid coolant temperatures both at the fixed axial mesh points and at moving points near the liquid-bubble interfaces. Axial heat conduction through the interfaces is ignored in the calculation of the interface liquid temperatures, so the calculated interface liquid temperatures actually correspond to the temperatures far enough from the interfaces so that axial heat conduction is negligible.

The calculation of the interface liquid temperature $T_{ci}(t+\Delta t)$ by a Lagrangian formulation is straightforward, since the total time derivative corresponds to the changes seen by an observer moving with the interface. Equation (109) is approximated by

$$\bar{\rho}\bar{c}\frac{T_{ci}(t+\Delta t) - T_{ci}(t)}{\Delta t} = \frac{\gamma}{2}[\varphi_1 - \bar{h}_2 T_{ci}(t+\Delta t) - \bar{h}_1 T_{ci}(t)] + \bar{Q}_c \tag{112}$$

where φ_1, $\bar{h}_1$, and $\bar{h}_2$ are now defined as

$$\varphi_1 = \frac{T_{ei}(t+\Delta t)}{R_{eci}(t+\Delta t)} + \frac{T_{ei}(t)}{R_{eci}(t)} + \gamma_2\left[\frac{T_{si}(t+\Delta t)}{R_{sci}(t+\Delta t)} + \frac{T_{si}(t)}{R_{sci}(t)}\right]$$

$$\bar{h}_1 = \frac{1}{R_{eci}(t)} + \frac{\gamma_2}{R_{sci}(t)}$$

and

$$\bar{h}_2 = \frac{1}{R_{eci}(t+\Delta t)} + \frac{\gamma_2}{R_{sci}(t+\Delta t)}$$

$$\gamma = \frac{surface\ area\ of\ cladding}{volume\ of\ coolant}$$

$$\gamma_2 = \frac{surface\ area\ of\ structure}{surface\ area\ of\ cladding}$$

The subscript i on T_{ei}, T_{si}, R_{eci}, and R_{sci} refers to values at the interface. Since the cladding and structure temperatures are only calculated at the fixed axial mesh points, T_{ei} and T_{si} are obtained by linear interpolation from the mesh-point values. The values of $\bar{\rho}$ and $\bar{c}$ are obtained using the extrapolated interface temperature at $t+\frac{1}{2}\Delta t$. Since direct heating of the coolant is normally a small effect, $\bar{Q}_c$ is obtained from the value at the nearest axial node.

Equation (112) is solved for $T_{ci}(t+\Delta t)$:

$$T_{ci}(t+\Delta t) = \frac{T_{ci}(t)(1-d_1\bar{h}_1) + d_1[\varphi_1 + (2\bar{Q}_c/\gamma)]}{1+d_1\bar{h}_2} \qquad (113)$$

where

$$d_1 = \frac{\gamma \Delta t}{2 \bar{\rho} \bar{c}} \tag{114}$$

The Lagrangian calculations for the coolant temperatures at fixed axial mesh points are similar to Eq. (113) :

$$T_c(z, t+\Delta t) = \frac{T_c(z-\Delta z, t)(1 - d_1 \bar{h}_1) + d_1[\varphi_1 + (2\bar{Q}_c/\gamma)]}{1 + d_1 \bar{h}_2} \tag{115}$$

where Δz is given by Eq. (111), d_1 is again given by Eq. (114),

$$\bar{\rho} = \bar{\rho}(z)$$

$$\bar{c} = \bar{c}(z)$$

$$\bar{Q}_c = \bar{Q}_c(z)$$

$$\varphi_1 = \frac{T_e(z, t+\Delta t)}{R_{ec}(z, t+\Delta t)} + \frac{T_e(z-\Delta z, t)}{R_{ec}(z, t)} + \gamma_2 \left[\frac{T_s(z, t+\Delta t)}{R_{sc}(z, t+\Delta t)} + \frac{T_s(z-\Delta z, t)}{R_{sc}(z, t)} \right] \tag{116}$$

and the temperatures $T_c(z - \Delta z, t)$, $T_e(z - \Delta z, t)$, and $T_s(z - \Delta z, t)$ are obtained by linear interpolation from the values at the fixed mesh points.

6. Heat Flow through Liquid-vapor Interface

SOBOIL model for calculation of interfacial heat transfer between liquid and vapor is

directly based on the work by Cronenberg et al.[2]. In this method, the total heat flow through the liquid-vapor interfaces is the sum of an upper interface term Iiu and a lower interface term I_{il}

$$E_i = \Delta t\left(I_{iu} + I_{il}\right) \tag{117}$$

where

$$I_{ix} = k_\ell A_{cx} \frac{\overline{\partial T_{\ell x}}}{\partial \xi}_{\xi=0} \tag{118}$$

with

x = u or ℓ

A_{cx} = Area of coolant channel

$T_{\ell x}$ = Liquid temperature near interface

k_ℓ = Liquid thermal conductivity near interface

ξ = Axial distance from interface

ξ = z - z_i for upper interface

ξ = - (z – z_i) for lower interface

and

$\frac{\overline{\partial T_{\ell x}}}{\partial \xi}$ is the time average of the spatial derivative for the time step

An expression for the coolant temperature derivative $\frac{\overline{\partial T_{\ell x}}}{\partial \xi}$ can be derived from the general heat conduction

$$\alpha \frac{\partial^{2T}{}_2(\xi, t')}{\partial \xi^2} + \frac{Q(\xi, t')}{\rho_2 C_2} = \frac{\partial T_\ell(\xi, t')}{\partial t'} \tag{119}$$

whre

α = $k_\ell / \rho_\ell C_\ell$, the thermal diffusivity of liquid sodium

k_ℓ = liquid thermal conductivity near interface

c_ℓ = liquid heat capacity

ρ_ℓ = liquid density

Q = heat input per unit volume in the liquid

T_ℓ = temperature in liquid slug

ξ = distance into liquid slug from liquid-vapor interface

and

t' = time since the vapor bubble started to form

The heat input Q includes both the direct heating Q_c and the heat flow $Q_{ec} + Q_{sc}$ from the cladding and structure to the liquid slug:

$$Q = Q_c + Q_{ec} + Q_{sc} \tag{120}$$

The boundary conditions for the problem are

$T_\ell(\xi = 0,\ t') = T(t')$, the liquid temperature at the liquid-vapor interface

and

$T_\ell(\xi = \infty,\ t') < \infty,$

and the initial condition is

$T_\ell(\xi, t' = 0)$ *known*

The heat conduction equation, Eq. (111), together with the initial and boundary conditions, can be solved for T_ℓ through the use of the Laplace transform method. The details of this approach is quite complex and tedious so that the results are represented in this report.

The final expression for heat fluxes at the interface are

$$I_{ix} = \frac{k_\ell}{\sqrt{\pi}} A_{cx} \frac{4}{3} \left[\bar{g}_x(t) \left(\frac{(t+\Delta t-t_b)^{3/2} - (t-t_b)^{3/2}}{\Delta t} - \sqrt{\Delta t} \right) \right.$$
$$+ \sqrt{\Delta t} \left(\frac{\gamma}{2} \left[\frac{T_{ex}(t) + T_{ex}(t+\Delta t) - T(t) - T(t+\Delta t)}{R_{ecx}} \right. \right.$$
$$\left. + \gamma_2 \frac{T_{sx}(t) + T_{sx}(t+\Delta t) - T(t) - T(t+\Delta t)}{R_{scx}} \right] \frac{\sqrt{\alpha}}{k_\ell} \qquad (121)$$
$$\left. \left. - \frac{1}{\sqrt{\alpha}} \frac{T(t+\Delta t) - T(t)}{\Delta t} \right) \right]$$

$$= \frac{4}{3} \frac{k_\ell}{\sqrt{\pi}} A_{cx} \bar{g}_x(t) \left(\frac{(t+\Delta t-t_b)^{3/2} - (t-t_b)^{3/2}}{\Delta t} - \sqrt{\Delta t} \right)$$
$$+ \frac{2}{3} \frac{\sqrt{\alpha}}{\sqrt{\pi}} \gamma \sqrt{\Delta t}\, A_{cx} \left[\frac{T_{ex}(t) + T_{ex}(t+\Delta t) - 2T(t)}{R_{ecx}} \right.$$
$$\left. + \gamma_2 \frac{T_{sx}(t) + T_{sx}(t+\Delta t) - 2T(t)}{R_{scx}} \right]$$
$$- \Delta T \left[\frac{2}{3} \frac{\sqrt{\alpha}}{\sqrt{\pi}} A_{cx} \sqrt[4]{\Delta t} \left(\frac{1}{R_{ecx}} + \frac{\gamma_2}{R_{scx}} \right) \frac{4}{3} \frac{k_\ell}{\sqrt{\pi}} \frac{A_{cx}}{\sqrt{\alpha}} \frac{1}{\sqrt{\Delta t}} \right]$$

where T(t + Δt) = T(t) + ΔT. Therefore the total heat flow through the liquid-vapor interfaces, gives

$$E_i = (I_{i0} + I_{i1}\, \Delta T)\, \Delta t \qquad (122)$$

where

$$I_{i0} = \frac{k_\ell}{\sqrt{\pi}} \left\{ \sum_{x=u,\ell} A_{cx} \left[\frac{2}{3} \frac{\sqrt{\alpha}}{k_\ell} \gamma \sqrt{\Delta t} \left[\frac{T_{ex}(t) + T_{ex}(t+\Delta t) - 2T(t)}{R_{ecx}} \right. \right. \right.$$
$$\left. + \gamma_2 \frac{T_{sx}(t) + T_{sx}(t+\Delta t) - 2T(t)}{R_{scx}} \right] \qquad (123)$$
$$\left. \left. + \frac{4}{3} \bar{g}_x(t) \left[\frac{(t+\Delta t - t_b)^{3/2} - (t-t_b)^{3/2}}{\Delta t} - \sqrt{\Delta t} \right] \right] \right\}$$

$$I_{i1} = \frac{k_\ell}{\sqrt{\pi}} \frac{4}{3} \sqrt{\Delta t} \left\{ -\frac{1}{\Delta t \sqrt{\alpha}} (A_{cu} + A_{c\ell}) - \frac{\gamma}{2k_\ell} \sqrt{\alpha} \left[\sum_{x=u,\ell} A_{cx} \left(\frac{1}{R_{ecx}} + \frac{\gamma_2}{R_{scx}} \right) \right] \right\}. \qquad (124)$$

This completes the task of expressing the heat flow through the interfaces as a linear function of the advanced time vapor temperatures.

7. Change in Vapor Energy

The heat flow into the bubble control volume is used both to produce new vapor and to raise the temperature of already existing vapor. During a time interval Δt, the vapor temperature goes from T to T+ΔT, the pressure goes from P_V+ΔP, the density goes from ρ_V+ $\Delta\rho_V$, the bubble volume goes from V_v to V_v+ ΔV, and the vapor energy changes by ΔE. The changes $\triangle$P and $\triangle\rho_v$ are related to $\triangle$T by the requirement that saturation conditions prevail in the vapor.

Two processes contribute to energy change $\triangle$E. One is the heating of the quantity of vapor present at the beginning of the time step from temperature T to temperature T+$\triangle$T. The other is the vaporizing of some of the liquid film to from additional vapor, giving a total vapor mass of (ρ_v + $\triangle\rho_v$) (V_v+$\triangle$V) at the end of the time step. However, it is not straightforward to formulate an expression for the energy change by directly considering the heating of the vapor (because of the volume and density changes which take place during the heating) and the vaporization of some liquid film (because the amount of film vaporized is unknown). Therefore, a thermodynamically equivalent path is flowed which does allow straightforward expression of the energy change. This path can be described in the following

three steps:

Step 1: condense the vapor in the bubble at time t to liquid at constant pressure and temperature:

$$\Delta E(1) = -(\rho_v V_v)\lambda \tag{125}$$

Where is the heat of vaporization at time t and

$$V_v = \int A_c \, dz$$
$$= A_c(JST)\Delta z'(JST) + \sum_{JC=JST+1}^{JEND-1} A_c(JC)\Delta z(JC) + A_c(JEND)\ \Delta z'(JEND) \tag{126}$$

Refer to Fig. 3.2-1 for the notation.

Step 2 : heat the liquid from step 1 to T+△T:

$$\Delta E(2) = C_\ell(\rho_v V_v)\Delta T \tag{127}$$

Where C_l is the capacity of the liquid and the compressibility of the liquid is neglected.

Step 3 : vaporize the liquid from step 2 plus enough liquid from the film to fill the volume V_v+△V:

$$\Delta E(3) = (\rho_v + \Delta\rho_v)(V_v + \Delta V)(\lambda + \Delta\lambda) \tag{128}$$

If the vapor undergoes a not energy loss rather than a gain, the liquid in Step 2 shows a temperature drop of △T and part of the vapor in Step 3 condenses onto the cladding and/or structure.

The energy change is then

$$\Delta E = \Delta E(1) + \Delta E(2) + \Delta E(3) \tag{129}$$

or, neglecting second-order terms,

$$\Delta E = \rho_v V_v \Delta\lambda + \rho_v \lambda \Delta V + \lambda V_v \Delta\rho_v + \rho_v V_v C_\ell \Delta T. \tag{130}$$

Now, the energy change must be expressed as a linear function of the change in vapor temperature $\triangle$T. To do this, first look at the volume change $\triangle$V. this term is currently modeled as the change in volume at the liquid-vapor interfaces due to interface motion, neglecting any volume change due to flow area changes caused by cladding motion during the time step. Accordingly, using earlier notation, $\triangle$V for bubble K is just

$$\begin{aligned}\Delta V = &\left[A_{c\ell}(t+\Delta t)\ z_i(1,t+\Delta t,K) - A_{c\ell}(t)\ z_i(1,t,K)\right] \\ &+ \left[A_{cu}(t+\Delta t)\ z_i(2,t+\Delta t,K) - A_{cu}(t)\ z_i(2,t,K)\right]\end{aligned} \tag{131}$$

The flow area A_C at the interfaces is written as a time-dependent function to account for the possibility that an interface might cross from one mesh segment to another during the time step. Since the flow area can vary from mesh segment to mesh segment, this might in a change in interface flow area from t to t+$\triangle$t.

To simplify the expression for $\triangle$V, define an average interface area at the lower interface as

$$\bar{A}_c(K,1) = \frac{A_{c\ell}(t+\Delta t)z_i(1,\ t+\Delta t,\ K) - A_{c\ell}(t)z_i(1,\ t,\ K)}{z_i(t,\ t+\Delta t,\ K) - z_i(1,\ t,\ K)} \tag{132}$$

A similar definition can be made at the upper interface. Then $\triangle$V becomes

$$\begin{aligned}\Delta V = &\ \bar{A}_c(K,2)\left[z_i(2,\ t+\Delta t,K) - z_i(2,t,K)\right] \\ &- \bar{A}_c(K,1)\left[z_i(1,t+\Delta t,K) - z_i(1,t,K)\right]\end{aligned} \tag{133}$$

The advanced time interface positions Z_i(L, t+$\triangle$t, K) can be expressed in terms of the changes in pressure at the interfaces via Eq. 3.5-22 to give

$$\begin{aligned}\Delta V &= \Delta V_0 + \bar{A}_c(K,2)\Delta z'(K,2) - \bar{A}_c(K,1)\Delta z'(K,1) \\ &= \Delta V_0 + \bar{A}_c(K,2)\frac{dz_i(K,2)}{dp}(\Delta p_K - \Delta p_{K+1}) \\ &\quad - \bar{A}_c(K,1)\frac{dz_i(K,1)}{dp}(\Delta p_{K-1} - \Delta p_K)\end{aligned} \tag{134}$$

where

$$\Delta V_0 = \bar{A}_c(K,2)\Delta z_0(K,2) - \bar{A}_c(K,1)\Delta z_0(K,1) . \tag{135}$$

Using Eq. 3.5-77 in Eq. 3.5-73 for the energy change $\triangle$E produces an expression for $\triangle$E in terms of the changes in , p_V, and p_V as well as T. To reduce this to a linear equation in $\triangle$T, the changes in , p_V, and p_V are approximated by

$$\Delta\lambda = \Delta T\frac{d\lambda}{dT} \tag{136}$$

$$\Delta\rho_v = \Delta T\frac{dp_v}{dT} \tag{137}$$

and

$$\Delta P = \Delta T\frac{dP_v}{dT} \tag{138}$$

Where the temperature derivatives are evaluated along the saturation curve. Incorporating Eqs. 3.5-79 into Eq. 3.5-73 results in a formulation for the change in energy within the control volume which is a linear function of $\triangle$T:

$$\Delta E = \Delta E_0 + \Delta E_1\Delta T(K) + \Delta E_2\Delta T(K+1) + \Delta E_3\Delta T(K-1) \tag{139}$$

where

$$\Delta E_0 = \lambda \rho_v \Delta V_0$$

$$\Delta E_1 = \lambda \left\{ \rho_v \frac{dp(K)}{dT} \left[\bar{A}_c(K, 1) \frac{dz_i(K, 1)}{dp} + \bar{A}_c(K, 2) \frac{dz_i(K, 2)}{dp} \right] + (V_v + \Delta V_0) \frac{d\rho_v}{dT} \right\} + \rho_v \Delta V_0 \frac{d\lambda}{dT} + \rho_v V_v C_\ell$$

$$\Delta E_2 = 0 \quad if \; K = K_{vm} = \text{last bubble in channel}$$

and otherwise,

$$\Delta E_2 = -\rho_v \lambda \bar{A}_c(K, 2) \frac{dz_i(K, 2)}{dp} \frac{dp(K + 1)}{dT} ;$$

$$\Delta E_3 = 0 \; if \; K = 1 .$$

and otherwise,

$$\Delta E_3 = -\rho_v \lambda \bar{A}_c(K, 1) \frac{dz_i(K, 1)}{dp} \frac{dp(K - 1)}{dT}$$

8. Energy Balance

As discussed at the beginning of this section, an energy balance exists between the energy transferred to the control volume and the change in energy within the volume. The change in energy is given by Eq. 3.5-80, derived in the previous subsection. The energy transferred to the volume, Et, is the sum of the energy flow from the cladding and structure, E_{es}, and the energy flow through the liquid-vapor interfaces, Ei; this was expressions for E_{es} and Ei derived in energy transferred to the control volume as

$$E_t = E_{t0} + E_{t1}\Delta T(K) + E_{t2}\Delta T(K + 1) + E_{t3}\Delta T(K - 1) \qquad (140)$$

where

$$E_{t0} = \Delta t\left[\frac{Q_{es}(K,t) + I_{e1}(K)}{2} + I_{i0}\right]$$

$$E_{t1} = \Delta t\left[\frac{I_{e2}(K)}{2} + I_{i1} + \frac{I_{e3}(K)}{2}\frac{dz_i(K,2)}{dp}\frac{dp(K)}{dT} - \frac{I_{e4}(K)}{2}\frac{dz_i(K,1)}{dp}\frac{dp(K)}{dT}\right]$$

$$E_{t2} = 0 \;\; if \;\; K = K_{vn}$$

and otherwise,

$$E_{t2} = -\frac{\Delta t}{2} I_{e3}(K)\frac{dz_i(K,\,2)}{dp}\frac{dp(K+1)}{dT}$$

$$E_{t3} = 0 \;\; if \;\; K = 1$$

and otherwise,

$$E_{t3} = \frac{\Delta t}{2} I_{e4}(K)\frac{dz_i(K,\,1)}{dp}\frac{dp(K-1)}{dT}\,.$$

The overall energy balance is then

$$E_t = \Delta E$$

If the expression for Et from Eq. 3.5-85 and that for △E. 3.5-80 are inserted into Eq. 3.5.90, the result is a linear equation in terms of the changes in the vapor temperatures of bubbles K-1, K, and K+1:

$$C_4(K) + C_1(K)\Delta T(K) + C_2(K)\Delta T(K+1) + C_3(K)\Delta T(K-1) = 0 \qquad (141)$$

where

$$C_4(K) = \Delta E_0(K) - E_{t0}(K)$$

$$C_1(K) = \Delta E_1(K) - E_{t1}(K)$$

$$C_2(K) = \Delta E_2(K) - E_{t2}(K)$$

$$C_3(K) = \Delta E_3(K) - E_{t3}(K).$$

9. Vapor Temperatures

Equation 3.5-91 can be written for each uniform pressure bubble in the channel. The equations are then solved for the changes in vapor temperature for each bubble as follows. First, each bubble in the channel is checked in order from the bottom of the channel to the top to determine whether it is a uniform-pressure or variable - pressure bubble. This determines how uniform - pressure bubbles are distributed throughout the channel and allows the temperature calculation to be carried out simultaneously for all bubbles that are in any one group of bubble (e.g., if the lowest bubble in the channel is a large, pressure-gradient bubble with four small constant pressure bubbles above it, the temperatures in the four small bubbles will be computed simultaneously). In general, if a series of N bubbles of uniform vapor pressure extends from bubble K_b to bubble K_t, then the temperatures in the N bubbles are calculated by solving a set of linear equations will be written in terms of N unknowns if $\triangle T(K_b-1)$ are $\triangle T(K_t+1)$ are set to extrapolated values (or to zero, if $K_b=1$ or $K_t=K_{VN}$) and the coefficient C_4 is modified to be

$$C_4(K_b) \rightarrow C_4(K_b) + C_3(K_b)\Delta T(K_b - 1), \; if \; K_b > 1 \tag{141}$$

$$C_4(K_t) \rightarrow C_4(K_t) + C_2(K_t)\Delta T(K_t + 1), \; if \; K_t < K_{vN} \tag{142}$$

The N equations are then solved using Gaussian elimination. After the bubble temperatures

are obtained, the saturation conditions are used to obtain the bubble pressures.

Chapter 2 SOBOIL Structure

1. Overview of Basic Calculation Logic

SOBOIL consists of several key subroutines. First it reads input variables that users must supply for the calculation. These are geometric data, some information necessary for numerical method, i.e. time-step, implicitness, channel inlet temperature, critical temperature of sodium, initial junction temperature, and so on. Inputs necessary for fuel temperature calculation also must be supplied.

After it reads those input variables, it defines various common or local variables. At the same time, it also initializes the variables which are updated with time. They include logical variables as well as numerical variables. The logical variables are represented by total number of bubbles in the channel (KB), indication of a bubble existence in a volume(NOBUB), initial bubble or not (INITB), etc. The real variables are those of top and bottom bubble pressures together with temperatures of the liquid slugs, interfacial velocities, vapor volume, wall heat transfer rate, so on. The first calculation is to determine the junction positions based on the input node numbers and channel lengths. Liquid only flow is assumed in the channel initially.

As a transient starts, it searches whether a bubble has existed or not. If a bubble has already existed, it replaces the upper and bottom vapor pressures and pressure increments. Then, it calls 'SLTEMP' for the temperature distributions in the liquid slug. It also calculates the slug flow rates as well as pressure distributions within the liquid slugs with saturation temperatures by calling the subroutine, 'LIQSLUG'. It checks, then, whether a bubble is the initial bubble or not. If the bubble is the initial bubble, the maximum temperature in the liquid slug is searched to determine the bubble generation condition. In case that the maximum temperature exceeds the super heating temperature specified by a user, iteration is made to find out the exact boiling time with reducing the time step size. At this time the liquid flow rates keep the same values, however, the liquid temperature distribution is repeatedly calculated until the superheat lies within some user specified criteria. When a new bubble is generated, it corrects bubble numbers, defines the bubble generation time, and updates the flag for the new bubble, newly order the bubble serial numbers to take account of the new total number of bubbles. It assumes that the bubble temperature were the

superheated temperature of the liquid at boiling and the bubble pressure to be the saturation pressure at the bubble temperature.

Subsequently, it calculates the initial volume change for the new bubble and the interface positions (upper and lower) for the bubble. The wall heat fluxes into the bubbles except the new bubble are then estimated. The interfacial heat transfer and bubble positions are also improved sequentially. After all heat transfer rates and new positions are calculated, vapor bubble temperatures are obtained by solving the linear algebraic equation for the vapor bubbles. The new variables are replaced as previous variables for the next time step.

2. Algorithm

These overall calculation logic is summerized as follows :

< Initializations and Definitions >

1. Read input as guided in Input Manual
2. Initialize the necessary variables
3. Calculate channel inlet temperature as a function of time
4. Calculate node junction height using user defined mesh sizes

< Slug calculation >

1. Check if there is a bubble in the channel or not ?
2. SLUG = 10, 9, ... 1

(1) Determine integers for JSLUG(ICH,KBUB,1) and JSLUG(ICH,KBUB,2)

- If no condition for a bubble formation in a node, then go to next time step

(2) Calculate coolant temp. profile

- ♦ Determine maximum junction temp. and the position where it occurs
- ♦ If a liquid slug locates within a volume, go to 600
  - No slug temp. calculation. Otherwise, calculation of temp. profile within the slug

(3) Calculate liquid flow rate and pressure profile in the channel

(4) Calculate saturation temp. under the pressure at the junction of the maximum temp.

(5) Check if the maximum coolant temp. exceed the user defined superheated

temperature for an initial bubble formation or not. Otherwise, go to the next time step.

♦ if the saturation temp. gets higher than the specified value for bubble formation, then

- Reduce the time step until

  ABS($T_{j,max} - (T_{sat} + \Delta T)$) < 0.005 should be satisfied

- When the condition is met, a initial bubble is formed
  - add one bubble
  - $P_v = P_{sat}(T_{sat} + \Delta T)$
  - $P_t = P_v$
  - $P_b = P_b$

(6) go to 'a new bubble formation'

< For other bubbles than the initial bubble >

1. Calculation of liquid slug flow rate and pressure profile below the bubble
2. Calculation of saturation temp. under the pressure at the maximum coolant temp.
3. If $T_{j,max} > (T_{sat} + \Delta T)$ is met, then
   - Additional bubble formation
   - $P_v = P_{sat}(T_{sat} + \Delta T)$
   - $P_t = P_v$
   - $P_b = P_b$
4. go to 'a new bubble formation'

< Bubble calculation >

KBUB = 9, 8, ..., 2, 1

1. Wall heat transfer into the bubble(s)
2. Interface heat transfer at bubble interfaces
3. Calculations of new bubble locations (Z_{i1}(KBUB,L), Interfacial velocity, ..)

- Does a bubble flow out at the channel ?
- Does a bubble collapse ?
- NKBUB → NKBUB-1
- Reordering of bubbles
- Replacement of all relevant variables

4. Bubble energy equation solving (Tri-diagonal matrix)
5. Update bubble conditions

< New bubble formation >

1. Determination of the new bubble location
2. Update bubble ordering
3. Definition of the new bubble temp. and pressure
4. Determine node locations of upper and lower interfaces of the liquid Slug
5. Replacement all relevant variables
6. Determine initial bubble volume ($r = 2\sigma/\Delta P$)
7. Calculating locations of upper and lower interfaces for the new bubble

< Advancement of time >

1. Advancement of time
2. Update fuel rod temp. distributions
3. Update junction and volume temp. for the next calculation
4. Update all relevant variables
6. If time does not reach the termination time, then go to 'Slug calcualtion'.
7. Stop
8. End

This logic is also illustrated in Fig. 8 (1), (2).

Fig. 9 illustrates the flow logic for temperature calculation in SLTEMP. The basic input variables for SLTEMP are a channel number, a liquid slug number, total number of bubbles, and geometrical data. It also needs additional variables such as the liquid flow rate, the position of liquid slug, etc. The physical properties in the node volumes are estimated based on the temperatures at the previous time step. When bubbles exist in the channel, the node sizes for volumes where the liquid-vapor interfaces are located, are recalculated. The wall heat transfer coefficients between sodium and the heating structures are then calculated using Nusselt numbers from those of SAS2A model. As the marching scheme is used in 'SLTEMP', the next junction temperature is calculated based on the previous junction temperature so that the sequence of the calculation should be reversed when reversed flow is formed. Iteration for solving temperatures should be made until they converge because the initial temperatures are predictor step values. After the convergence it checks bubble existence as well as bubble distribution within the channel. In case that the bubbles are close enough not to form a bubble in a liquid slug, it generates the flag for unavailability of boiling. It always check the maximum temperature in the channel.

3. Flow Chart

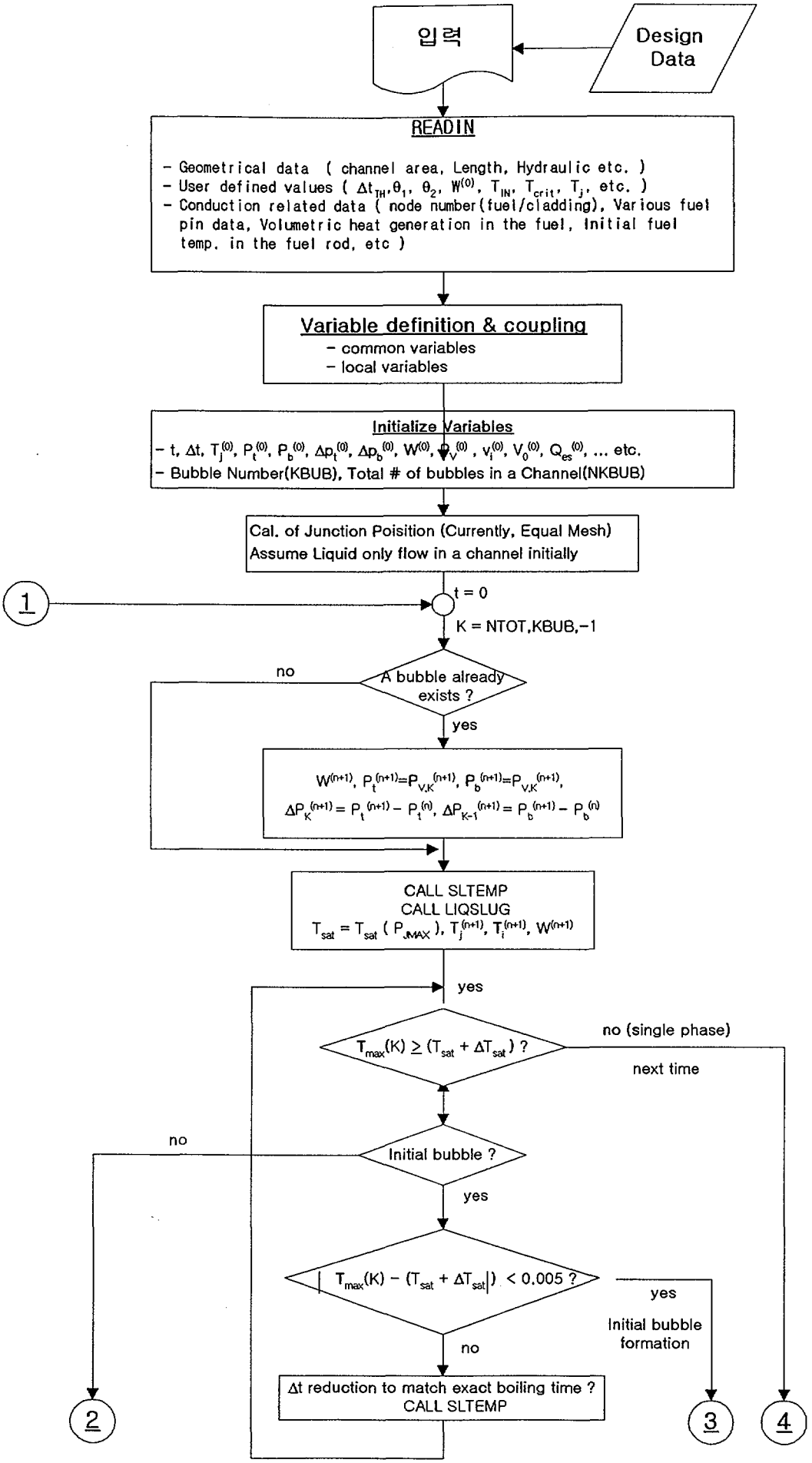

Fig. 8 (1) Flow Chart for SOBOIL

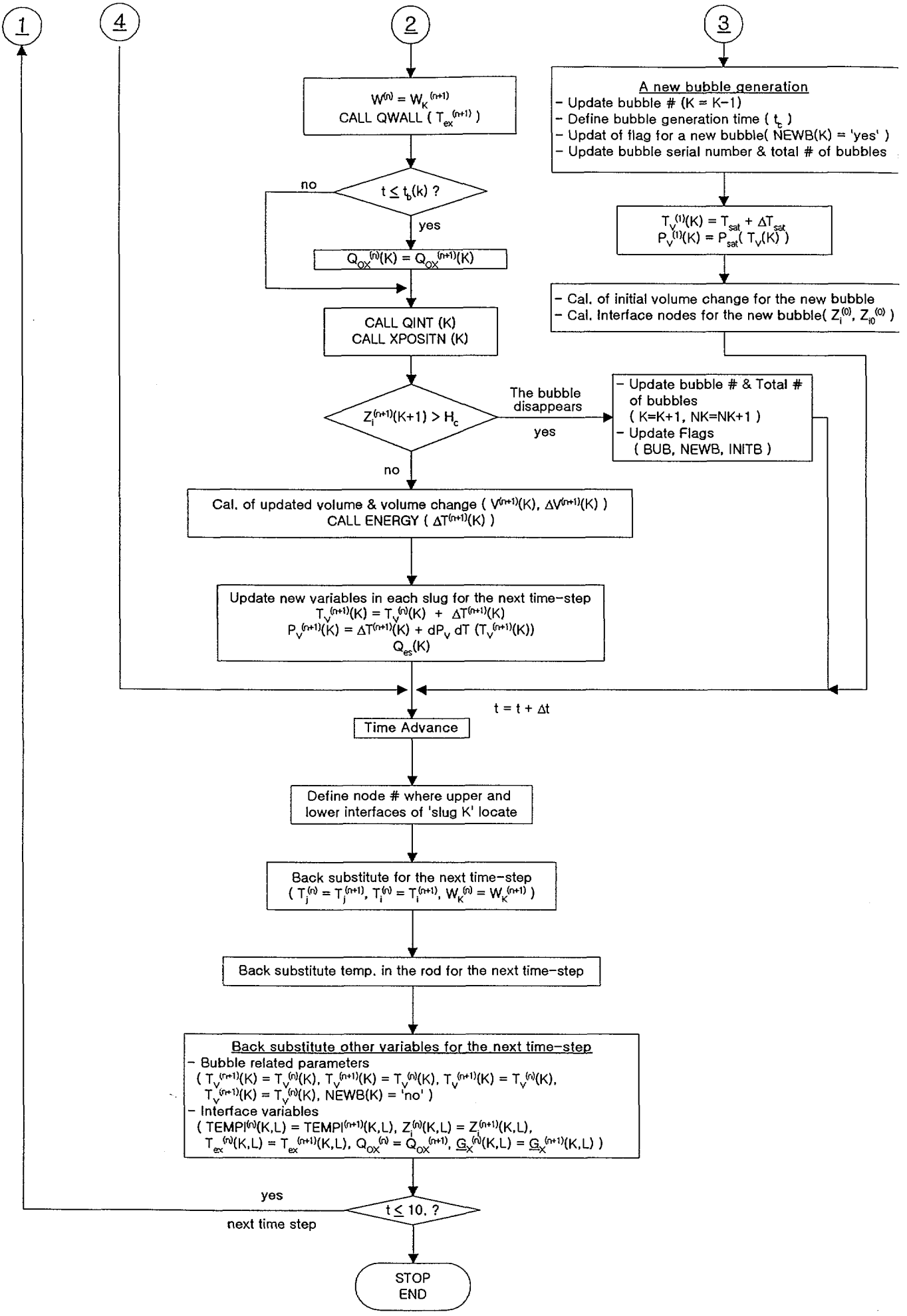

Fig. 8 (2) Flow Chart for SOBOIL

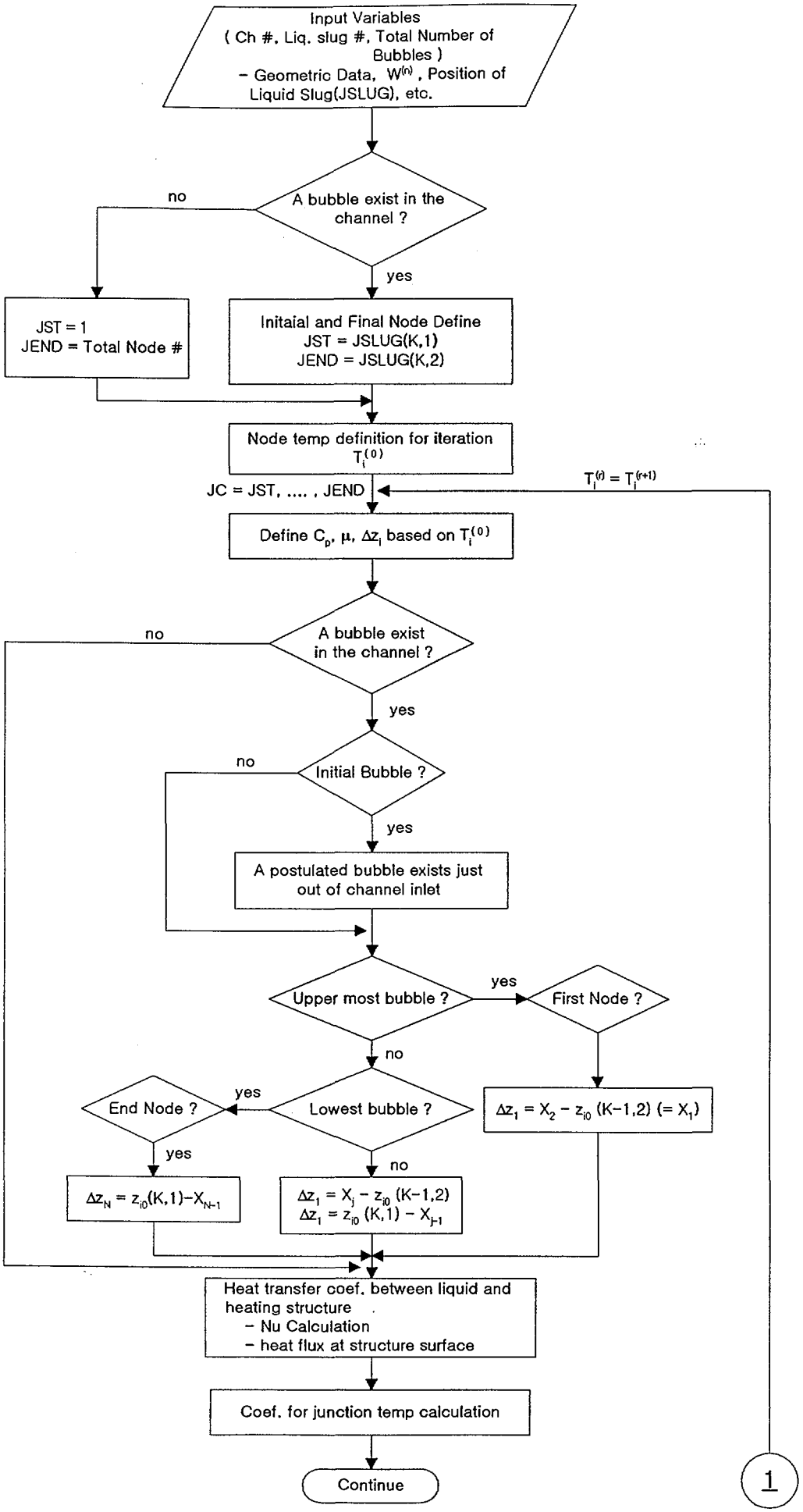

Fig. 9 Flow Chart for SLTEMP

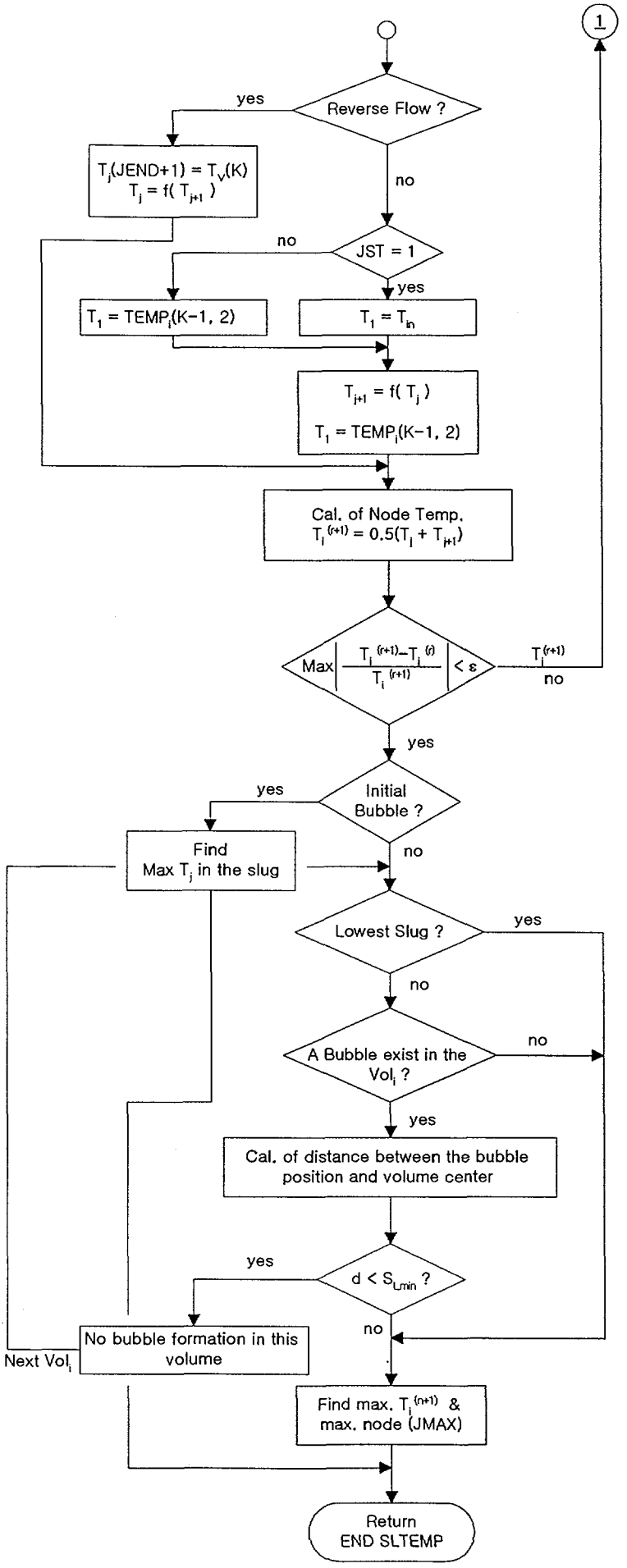
1
Reverse Flow ?
yes
no
$T_j(JEND+1) = T_V(K)$
$T_j = f(T_{j+1})$
JST = 1
no
yes
$T_1 = TEMP_i(K-1, 2)$
$T_1 = T_{in}$
$T_{j+1} = f(T_j)$
$T_1 = TEMP_i(K-1, 2)$
Cal. of Node Temp.
$T_i^{(r+1)} = 0.5(T_i + T_{i+1})$
Max $\left|\frac{T_i^{(r+1)} - T_i^{(r)}}{T_i^{(r+1)}}\right| < \varepsilon$
$T_i^{(r+1)}$
no
yes
Initial Bubble ?
yes
no
Find Max T_j in the slug
Lowest Slug ?
yes
no
A Bubble exist in the Vol_i ?
no
yes
Cal. of distance between the bubble position and volume center
$d < S_{L,min}$?
yes
no
No bubble formation in this volume
Next Vol_i
Find max. $T_i^{(n+1)}$ & max. node (JMAX)
Return
END SLTEMP

References

[1] Nuclear Development associates, "An Estimate of the Order of Magnitude of the Explosion When the Core of a Fast Reactor Collapses, " British Report UKAEA-RHM (56/113), Classified, 1956, and Nuclear Development Associates Report NDA-14-170, 1957

[2] G.A. Greene, T. Ginsberg, and M.S. Kazimi, "Assessment of the Thermal Hydraulic Technology of the Transition Phase of a Core-Disruptive Accident in a LMFBR", NUREG/CR-3014, Nov. 1982

[3] F.E. Dunn, et al., "The SAS2A LMFBR Accident-Analysis Computer Code," ANL-8183, Oct. 1974

[4] M. Green, "FRAX, A Whole Core Accident Code for Fast Reactors", AEA Presentations to KAERI, March 1998

[5] D.J. Brear, J.A. Moran, T. Rudge, "Fuel Pin loading and pin failure criteria in the UK code FRAX-5 under WCA condition", Fast Reactor Core and Fuel Structure Behavior, BNES, London, 1990

[6] T. Rudge, "Homsep-2 : A One-dimensional Sodium Boiling Model for the Fast Reactor", Nucl. Energy, 1989, 28, N0. 3, June, 171-181

User manual for SOBOIL

(Draft)

'98/08/21

KALIMER SAFETY ANALYSIS

KALIMER TECH. DEVELOPMENT TEAM

KOREA ATOMIC ENERGY RESEARCH INSTITUTE

Program 'SOBOIL' consists of following input variables. User should note that the sequence of input variables must be consecutive, otherwise there will be a problem to read the input. Error indication is not enough to find errors in the input lists easily at the present time and thus users should make sure of the card number and the number of input variables in a card. User also notes that units of all physical quantities should be given in **SI units.**

0. Title :
   - The character of the problem title should not exceed 80 characters and there is no need for a card number.

1. Total channel number to be considered
   1.0 NCHAN
   (1 integer)

   (a) NCHAN : Total number of the core channels to be analyzed

2. Geometric Inputs

Following card is repeated in NCHAN times

2.0 ICHAN, CHANAC(I), DHYDR(I), XLCHAN(I), NVOL(I), XKOR(I), PERI(I), PIDR(I)

(2 integer, 6 real numbers for each channel)

(a) ICHAN : Channel number (= 1, NCHAN)
(b) CHANAC(I) : Channel area (m^2)
(c) DHYDR(I) : Channel hydraulic diameter (m)
(d) XLCHAN(I) : Channel length (m)
(e) NVOL(I) : Total volumes in the channel
(f) XKOR(I) : Integrated loss coefficients in the channel
(g) PERI(I) : Perimeter of the coolant channel when it is assumed as circular tube
(h) PIDR(I) : Axial weighting factor for power generation in a fuel rod (Ratio of heat generated in the fuel to that in the coolant by direct heating)

3. Title

- The character of the problem title should not exceed 80 characters and there is no need for a card number.

4. Inputs for various conditions

4.0 DELT, THETA1, THETA2, WSLUG0, TEMPLIN, PRESIN, PRESOUT
(2 integers, 5 real numbers)

(a) DELT : Thermal-hydraulic time step [s]
(b) THETA1 : Implicitness factor (0 for fully implicit method, 1 for explicit method) ($0. \le \theta_1 \le 1.0$)
(c) THETA2 : Implicitness factor (1 for fully implicit method, 0 for explicit method) ($0. \le \theta_2 \le 1.0, \quad \theta_1 + \theta_2 = 1.0$)
(d) WSLUG0 : Initial channel flow rate [kg/s]
(e) TEMPLIN : Channel inlet coolant temperature (°C)
(f) PRESIN : Channel inlet coolant pressure (Pa)
(g) PRESOUT : Channel outlet coolant pressure (Pa)

4.1 TEND, SLMIN
(2 real numbers)

(a) TEND : Programe end time [s]
(b) SLMIN : Minimum distance between adjacent bubbles [m]

5. Title

- The character of the problem title should not exceed 80 characters and there is no need for a card number.

5.0 TCRIT, PCRIT
(2 real numbers)

(a) TCRIT : Convergence criteria for temp. calculation in 'TEMPL'
(b) PCRIT : Convergence criteria for pressure calculation in 'LIQSLUG'

6. Title

- The character of the problem title should not exceed 80 characters and there is no need for a card number.

6.0 C1, C2, C3
(3 real numbers)

(a) Coefficients for transient inlet temperature conditions
Y = C0 + C1*X + C2*X**2 + C3*X**3

7. Title

- The character of the problem title should not exceed 80 characters and there is no need for a card number.

7.0 ICHAN

(a) ICHAN : Channel number

7.1 JUNC, TEMPJ(ICH, NTOT, J) for J = JC, JC+NJ

(NJ integer, NJ real numbers)

(a) JUNC : Channel junction number
(b) TEMPJ(ICH, NTOT, J) : Junction initial temperature [°C]

8. Title

- The character of the problem title should not exceed 80 characters and there is no need for a card number.

8.0 NUM(0), JMOD
(2 integers)

(a) NUM(0) : Card identification number (= 0)
(b) JMOD : Scheme selection code (Semi-implicit/Fully implicit)

8.1 NUM(1), NP, NC
(3 integer)

(a) NUM(1) : Card identification number (= 1)
(b) NP : Node number of the fuel or structure
(c) NC : Node number of the cladding

8.2 NUM(2), RPZERO, RPOUT
(1 integer, 2 real numbers)
(a) NUM(2) : Card identification number (= 2)
(b) RPZERO : Inner radius of the fuel
(c) RPOUT : Outer radius of the fuel

If $NC \neq 0$
8.3 NUM(3), RECZERO, RCOUT
(1 integer, 2 real numbers)

(a) NUM(3) : Card identification number (= 3)
(b) RECZERO : Inner radius of the cladding
(c) RPOUT : Outer radius of the cladding

8.4 NUM(4), IAXAL, (VZEROIN(IAX, J), J=1, NP+NC)
(NCHAN*NVOL integer2, NCHAN*NVOL*(NP+NC) real numbers)

(a) NUM(4) : Card identification number (= 4)

(b) IAXAL : Axial node number of ICHAN
(c) VZEROIN(IAX,J) : Initial temperature at the radial nodes [K]

8.5 NUM(5), IBND, OBND
(3 integers)

(a) NUM(5) : Card identification number (= 5)
(b) IBND : Inner boundary condition flag (2 = specified heat flux, Otherwise convection boundary)
(c) OBND : Outer boundary condition flag (2 = specified heat flux, Otherwise convection boundary)

if IBND = 2
8.6 NUM(6), QFLUXIN
(1 integer, 1 real numbers)

(a) NUM(6) : Card identification number (= 6)
(b) QFLUXIN : Inner specified heat flux ($W/m^2 - K$)

8.7 QFLUXOUT
(1 real number)

(a) QFLUXOUT : Outer specified heat flux ($W/m^2 - K$)

8.8 NUM(7), ICHAN, QPIN
((NCHAN+1) integers, NCHAN real number2)

(a) NUM(7) : Card identification number (= 7)
(b) ICHAN : Channel number
(c) QPIN : Heat generation rate in the channel ICHAN [W]

8.9 JVOL, FPOW(ICH, I)
(NCHAN*NVOL integer, NCHAN*NVOL real numbers)

(a) JVOL : Node number of the channel ICHAN
(b) FPOW(ICH, I) : Heat generation rate in the volume JVOL in the channel ICHAN

If $NC \neq 0$
8.10 NUM(8), HGAP
(1 integer, 1 real number)

(a) NUM(8) : Card identification number (= 8)
(b) HGAP : Gap conductance between the fuel and cladding

부 록

(입력 예)

(1) Fuel pin data

```
1
1    1.102e-5    3.274e-3    1.0    20    10.0    0.001873    1.1278
```

(2) Common data

1.0e-3	0.	1.0	0.06933	1149.5	4.70e5	3.2e5
5.	0.02					

(3) Convergence Criteria for Temp. and Pressure

1.0E-6	1.0E-5

(4) Constants for transient

50.	0.	0.

(5) Channel junction temperatures

1

1	1149.5	2	1156.101	3	1162.666	4	1170.426
5	1178.142	6	1186.993	7	1195.870	8	1205.536
9	1215.195	10	1225.144	11	1235.092	12	1244.818
13	1254.511	14	1263.563	15	1272.616	16	1280.491
17	1288.360	18	1294.771	19	1301.176	20	1305.922
21	1310.670						

(6) Fuel rod conduction data

0 0

1 6 3

2 0. 2.9e-3

3 3.305e-3 3.835e-3

4 1

1	692.2	690.7	686.2	678.7	668.1	654.3	649.6	644.3	639.4
2	695.3	693.9	689.4	681.9	671.3	657.6	652.9	647.6	642.6
3	708.6	706.8	701.6	692.8	680.4	664.3	658.7	652.5	646.7
4	712.3	710.5	705.3	696.5	684.2	668.1	662.6	656.3	650.5
5	725.5	723.6	717.6	707.6	693.6	675.3	668.9	661.8	655.2
6	729.7	727.8	721.8	711.9	697.8	679.6	673.3	666.2	660.
7	740.8	738.7	732.2	721.5	706.3	686.4	679.5	671.8	664.5
8	745.4	743.3	736.9	726.1	710.9	691.2	684.3	676.5	669.3
9	752.4	750.2	743.6	732.6	717.0	696.8	689.7	681.7	674.2
10	757.1	754.9	748.4	737.4	721.9	701.7	694.6	686.6	679.1
11	760.2	758.1	751.7	741.	725.8	706.0	699.1	691.2	683.9
12	764.9	762.8	756.4	745.6	730.5	710.8	703.9	696.0	688.7
13	764.3	762.3	756.3	746.3	732.1	713.8	707.2	699.9	693.1
14	768.7	766.7	760.7	750.7	736.6	718.3	711.8	704.4	697.6
15	763.2	761.4	756.2	747.5	735.2	719.3	713.6	707.2	701.2
16	767.	765.3	760.1	751.4	739.1	723.2	717.5	711.1	705.2
17	758.6	757.2	752.9	745.8	735.8	722.7	718.1	712.9	708.0
18	761.8	760.4	756.1	749.0	739.	726.	721.3	716.1	711.2
19	750.9	750.	746.6	741.3	733.9	724.2	720.7	716.9	713.2
20	753.3	752.2	749.0	743.7	736.2	726.6	723.1	719.3	715.6

5 0 1

7 1 6976.554

1	0.04055	2	0.04055	3	0.0478	4	0.0478
5	0.05475	6	0.05475	7	0.05975	8	0.05975
9	0.0615	10	0.0615	11	0.0603	12	0.0603
13	0.0564	14	0.0564	15	0.0491	16	0.0491
17	0.0401	18	0.0401	19	0.0298	20	0.0298

8 1.324e5

BIBLIOGRAPHIC INFORMATION SHEET

Performing Org. Report No.	Sponsoring Org. Report No.	Standard Report No.	INIS Subject code
KAERI/TR-1580/2000			

Title / Subtitle	Development of Two-phase Flow Model, 'SOBOIL', for Sodium
Main Author	Dohee Hahn (Safety Analysis Technology Development / Liquid Metal Reactor Design Technology Development Team)
Researcher and Department	Won Pyo Chang, In Chul Kim, Young Min Kwon, Yong Bum Lee, Dohee Hahn (Dept. of KALIMER Safety Analysis Technology Development)

Publication Place	대 전	Publisher	KAERI	Publication Date	2000. 3
Page	135 p.	I11. & Tab	Yes(x), No( )	Size	26 cm.
Note					
Classified	Open(x), Restricted( ), Class Document		Report Type	RR (Research Report)	
Sponsoring Org.			Contract No.		

Abstract (15-20 Lines)

The objective of this research is to develop a sodium two-phase flow analysis model, 'SOBOIL', for the assessment of the initial stage of the KALIMER HCDA (Hypothetical Core Disruptive Accident). The 'SOBOIL' is basically similar to the multi-bubble Slug Ejection model used in SAS2A[1]. When a bubble is formed within the liquid slug, the bubble fills the whole cross section of the coolant channel except for a film left on the cladding or on the structure. Up to nine bubbles, separated by the liquid slugs. are allowed in the channel at any time.

Each liquid slug flow rate in the model is performed in 2 steps. In the first step, the preliminary flow rate in the liquid slug is calculated neglecting the effect of changes in the vapor bubble pressures over the time step. The temperature and pressure distributions, and interface velocity at the interface between the liquid slug and vapor bubble are also calculated during this process. The new vapor temperature and pressure are then determined from the balance between the net energy transferred into the vapor and the change of the vapor energy. The liquid flow is finally calculated considering the change of the vapor pressure over a time step and the calculation is repeated until specified elapsed time is met.

Continuous effort, therefore, must be made on the examination and improvement for the model to become reliable. To this end, much interest must be concentrated in the relevant international collaborations for access to a reference model or test data for the verification.

Subject keywords (About 10 words)	LMR, KALIMER, SOBOIL, Sodium Boiling, HCDA Analysis, Sodium Two-phase Flow

서 지 정 보 양 식					
수행기관보고서번호	위탁기관보고서번호	표준보고서번호	INIS 주제코드		
KAERI/TR-1580/2000					
제목 / 부제	안전해석 기술개발				
주저자 및 부서명	한 도 희 (액체금속로 설계기술개발팀/안전해석 기술개발)				
연 구 자 및 부 서 명					
장원표, 김인철, 권영민, 이용범, 한도희 (KALIMER, 안전해석)					
출 판 지	대 전	발행기관	한국원자력연구소	발행년	2000. 5
페 이 지	135 p.	도 표	있음(X), 없음( )	크 기	26 cm.
참고사항					
비밀여부	공개(X), 대외비( ), _급비밀	보고서종류	기술보고서		
연구위탁기관		계약번호			

초록 (15-20 줄내외)

본 연구는 KALIMER HCDA(Hypothetical Core Disruptive Accident) 초기단계를 평가하기 위한 소듐 이상유동 해석모델 ' SOBOIL'의 개발을 목적으로 한다. ' SOBOIL' 은 기본적으로 SAS2A[1]에 사용된 Multi-bubble Slug Ejection 모델과 유사하다. 이 모델에서는 기포가 발생하면 기포는 피복재 혹은 구조물의 얇은 액체막을 제외한 전체 유로 단면적을 채우며, 액체 Slug 에 의해 분리되는 것으로 가정한다. 한 유로 내에서는 최대 9 개까지의 기포가 동시에 존재하는 것을 허용한다.

이 모델에서 각 액체 Slug 유동량 계산은 2 단계로 수행되는 데, 첫 단계로 기포의 압력이 변하지 않는 것으로 가정하고 초기 유동량을 먼저 계산한다. 이 과정에서 액체 Slug 의 온도 및 압력 분포, 그리고 액체와 기포사이의 경계면 속도도 함께 계산된다. 다음으로 기포로 전달되는 순 에너지와 기포의 내부 에너지 변화의 균형으로부터 새로운 기포의 온도 및 압력이 계산된다. 새로운 기포압력을 이용하여 최종 액체 Slug 유동량을 구하여 계산을 반복한다.

향후 개발된 모델이 신뢰할 수 있는 예측모델로 발전하기 위해서는 상당기간의 시험과 개선을 통한 검증이 필요하다. 이를 위해 국내에서 부재한 검증 참조 모델 혹은 실험자료를 확보하기 위해 관련 국제협력에 더욱 관심을 기울여야 할 것으로 사료된다.

주제명키워드
(10 단어내외)

액체금속로, KALIMER, SOBOIL, 소듐비등, HCDA 분석, 소듐 이상유동